Insights into innate immune activation via PS-ASO–protein–TLR9 interactions

Adam J. Pollak [ID]*, Luyi Zhao, Timothy A. Vickers, Ian J. Huggins, Xue-Hai Liang [ID] and Stanley T. Crooke [ID]

Ionis Pharmaceuticals, Inc. Carlsbad, CA 92010, USA

ABSTRACT

Non-CpG PS-ASOs can activate the innate immune system, leading to undesired outcomes. This response can vary—in part—as a function of 2′modifications and sequence. Here we investigated the molecular steps involved in the varied effects of PS-ASOs on the innate immune system. We found that pro-inflammatory PS-ASOs require TLR9 signaling based on the experimental systems used. However, the innate immunity of PS-ASOs does not correlate with their binding affinity with TLR9. Furthermore, the innate immune responses of pro-inflammatory PS-ASOs were reduced by coincubation with non-inflammatory PS-ASOs, suggesting that both pro-inflammatory and non-inflammatory PS-ASOs can interact with TLR9. We show that the kinetics of the PS-ASO innate immune responses can vary, which we speculate may be due to the existence of alternative PS-ASO binding sites on TLR9, leading to full, partial, or no activation of the pathway. In addition, we found that several extracellular proteins, including HMGB1, S100A8 and HRG, enhance the innate immune responses of PS-ASOs. Reduction of the binding affinity by reducing the PS content of PS-ASOs decreased innate immune responses, suggesting that PS-ASO–protein complexes may be sensed by TLR9. These findings thus provide critical information concerning how PS-ASOs can interact with and activate TLR9.

INTRODUCTION

Phosphorothioate containing antisense oligonucleotides (PS-ASOs) are synthetic nucleic acids that function via Watson-Crick base pairing to cognate RNA. PS-ASOs can modulate levels of diverse cellular RNA targets and are highly effective in a therapeutic context (1,2). To best facilitate RNase H1 mediated RNA cleavage, PS-ASOs utilize a gapmer design with deoxyribonucleotides in the middle of the short oligonucleotide (oligo) (gap), which are flanked by 2′ modified nucleotides (wing) (3). The 2′ modifications, such as 2′-O-methyloxylethyl (2′MOE) and constrained ethyl (cEt), provide enhanced RNA binding and protection against nucleases. PS linkages are commonly used because they enhance protein binding to facilitate tissue targeting and also protect against nucleases thus improving pharmacokinetic and pharmacodynamic properties, in comparison to natural phosphodiester (PO) linkages (4). However, PS-ASO design is still evolving to maximize their therapeutic index (T.I.) and to support the growing list of ways they can alter gene expression (2).

While PS-ASOs are typically active and safe, certain PS-ASOs can induce undesired effects, including cytotoxicity and innate immune responses (5). While these problematic PS-ASOs can be easily identified and discarded during the discovery stage, it is important to understand the mechanism of these toxicities so that they can be intentionally avoided. We recently provided a step-by-step molecular mechanism that explains how some PS-ASOs produce cytotoxicity (6). These toxic PS-ASOs tend to bind more proteins, especially paraspeckle proteins, more tightly (7). This leads to RNase H1 dependent protein mis-localization to the nucleolus, followed by nucleolar stress and apoptotic cell death. In turn, we reported straightforward medicinal chemical solutions that dramatically mitigate this toxicity and increase the T.I. of PS-ASOs. This was accomplished by evaluating the structure-activity relationships (SAR) of various modifications that enhance the T.I. of PS-ASOs. Cytotoxicity was best mitigated with modifications at gap positions 2–3 of 2′MOE and cEt gapmer PS-ASOs. This work sets the stage for a new generation of PS-ASOs with anti-cytotoxicity modifications at specific sites and motivates us to better define the molecular mechanistic basis of innate immune activation that can be a property of some PS-ASOs.

Toll-like receptors (TLRs) 3, 7, 8 and 9 are endosomal-localized receptors that recognize specific nucleic acids and are capable of mounting an innate immune response (8–10). siRNA-based therapeutics can have similar undesired effects as TLR3 responds to double-stranded (ds) RNA while TLR7/8 can respond to single-stranded (ss) RNA (11). Sequences containing unmethylated cytosine-guanine (CpG)

*To whom correspondence should be addressed. Tel: +1 760 603 3893; Fax: +1 760 603 2600; Email: apollak@ionisph.com

motifs, present in bacteria and DNA viruses, yet suppressed to a low level in mammalian species, are potent ligands of TLR9 [12]. Recent structural studies have shed light on the complexity of PS-ASO–TLR9 activation [13], including evidence of a second ligand docking site [14], as well as diverse nucleic acid structures that can activate TLR9 [15,16]. TLR9 activation requires dimerization, in which one TLR9 protomer recognizes the CpG nucleotides while the other protomer binds to the phosphate backbone [13]. The trafficking and activation of TLR9 proceeds from the ER to the plasma membrane surface, finally arriving in endosomal structures in a highly regulated process [17,18]. The endosomal activation of TLR9 recruits myeloid differentiation of primary response gene 88 (*Myd88*), instigating a cascade of signaling pathways including the activation of nuclear factor kappa-light-chain-enhancer of activated B cells (NF-κB), resulting in the expression of pro-inflammatory signals [8].

Non-CpG PS-ASOs have also been shown to induce innate immune responses via the TLR9 pathway [19,20], yet a structural explanation of these processes is lacking; in addition, there is evidence that TLR9-independent processes can occur [21]. Importantly, these innate immune responses can be modulated via changes to PS-ASO length, sequence, backbone modification, and 2′ ribose modification [19,22,23]. However, there is neither a detailed mechanistic understanding of these effects nor a general medicinal chemical strategy to reduce innate immune activation. Furthermore, a basic understanding of non-CpG innate immune PS-ASO trafficking and TLR9 engagement is lacking. Interestingly, CpG PS-ASO–protein interactions have been shown to play a role TLR9 signaling. For example, PS-ASOs bound to either HMGB1 or Granulin can more productively activate TLR9 as a complex than with the PS-ASO administered alone [24–26]. Given the extent of known PS-ASO-plasma protein interactions [27], we have been interested to determine whether any other plasma protein–PS-ASO complexes play a role in innate immune activation and to understand the molecular events that are involved in this process. Notably, the roles of PS-ASO–protein interactions for non-CpG PS-ASO activation of TLR9 remain understudied and other proteins are likely to play important roles.

Here, we report that several non-CpG PS-ASOs of diverse sequence and structure elicit innate immune responses utilizing the same signaling pathway induced by CpG PS-ASOs. Interestingly, we find that these PS-ASOs display different kinetics of activation and this phenomenon is best explained by classifying the slower PS-ASOs as weaker partial agonists, as they still effectively traffic to and engage with TLR9, yet the engagement appears to be less productive. We also find that many PS-ASOs bind to TLR9 but are competitive antagonists. Our data suggest that agonist strength may be related to the particular positioning of PS-ASOs on TLR9. In addition, we find that PS-ASO–extracellular protein interactions can either inhibit or enhance innate immune responses. We identify novel proteins that enhance these innate immune responses and demonstrate that the PS-ASO–protein complexes are taken up by cells and traffic in endosomes with the PS ASOs potentially forming an activated PS ASO-extracellular protein–TLR9 complex. Over-

all, our results provide new mechanistic insights into the highly complex process by which some PS-ASOs serve as TLR9 agonists and induce an innate immune response and set the stage for future experiments to develop strategies to mitigate PS-ASO innate immune responses.

MATERIALS AND METHODS

Materials

PS-ASOs (Supplementary Table S1), reagents (Supplementary Table S2 and S3), siRNAs and primer probes (Supplementary Table S4), and antibodies (Supplementary Table S5) are listed in Supplementary Materials.

RNA preparation and qRT-PCR

Total RNA was prepared using a RNeasy mini kit (Qiagen) from cells grown in 96-well plates using the manufacturer's protocol. qRT-PCR was performed in triplicate using TaqMan primer probe sets as described previously [28]. Briefly, ∼50 ng total RNA in 5 μl water was mixed with 0.3 μl primer probe sets containing forward and reverse primers (10 μM of each) and fluorescently labeled probe (3 μM), 0.5 μl RT enzyme mix (Qiagen), 4.2 μl RNase-free water, and 10 μl of 2 × polymerase chain (PCR) buffer in a 20 μl reaction. Reverse transcription was performed at 48°C for 10 min, followed by 94°C for 10 min, and then 40 cycles of PCR were conducted at 94°C for 30 s, and 60°C for 30 s within each cycle using the StepOne Plus RT-PCR system (Applied Biosystems). The results were analyzed by the relative quantity (ddCt) method. The mRNA levels were normalized to the amount of total RNA present in each reaction as determined for duplicate RNA samples using the Ribogreen assay (Life Technologies).

Western analyses

Cell pellets were lysed by incubation at 4°C for 30 min in RIPA buffer (50 mM Tris–HCl, pH 7.4, 1% Triton X-100, 150 mM NaCl, 0.5% sodium deoxycholate and 0.5 mM ethylenediaminetetraacetic acid (EDTA)). Proteins were collected by centrifugation. Approximately 20–40 μg of protein were separated on 6–12% NuPAGE Bis-Tris gradient sodium dodecyl sulphate-polyacrylamide gel electrophoresis gels (Life Technologies) and transferred onto polyvinylidene difluoride (PVDF) membranes using the iBLOT transfer system (Life Technologies). The membranes were blocked with 5% non-fat dry milk in 1× PBS at room temperature for 30 min. Membranes were then incubated with primary antibodies at room temperature for 2 h or at 4°C overnight. After three washes with 1× PBS, the membranes were incubated with species appropriate HRP-conjugated secondary antibodies (1:2000) at room temperature for 1 h to develop the image using Immobilon Forte Western HRP Substrate (Millipore). Uncropped gels can be seen in Supplementary Figure S12.

Immunofluorescence staining, and confocal imaging

293-TLR9 cells grown in glass bottom dishes were washed with 1× phosphate-buffered saline (PBS), fixed with 4%

paraformaldehyde for 0.5–1 h at room temperature, and permeabilized for 4 min with 0.1% Triton in $1\times$ PBS. After blocking at room temperature for 30 min with 1 mg/ml bovine serum albumin (BSA) in $1\times$ PBS, cells were incubated with primary antibodies (1:100–1:300) in 1 mg/ml BSA in $1\times$ PBS for 2–4 h, washed three times (5 min each) with 0.1% nonyl phenoxypolyethoxylethanol-40 (NP-40) in $1\times$ PBS and incubated for 1 h with secondary antibody conjugated with fluorophores (1:200). After washing three times, cells were mounted with anti-fade reagent containing DAPI (Life Technologies). Bjab cells were first attached to glass-bottomed dishes coated with polylysine before the above procedure was taken. Images were acquired using confocal microscope (Olympus FV-1000) and processed using FV-10 ASW 3.0 Viewer software (Olympus). For live-cell imaging, attached Bjab cells treated with indicated PS-ASOs were treated with Lysotracker Green DND-26 (Life Technologies) per the manufacturer's instructions. Indicated proteins were labeled with Alexa-647 via the Alexa Fluor 647 Microscale Labeling kit (Life Technologies) per the manufacturer's instructions, prior to incubation with cells.

Cell culture

HEK-Blue™ hTLR9 cells (Invivogen) (293-TLR9) and THP1-Dual™ hTLR9 cells (Invivogen) (THP1-TLR9) are stable commercial cell lines that co-expresses the TLR9 gene and an optimized secreted embryonic alkaline phosphatase (SEAP) reporter gene in HEK293 or THP1 cells. This SEAP reporter gene is controlled by IFN-β promotor fused to five NF-κB and AP-1 binding sites. With TLR9 ligand stimulation, NF-κB and AP-1 are induced to produce SEAP.

293-TLR9 cells were grown according to manufactures' instruction in a maintenance media of Dulbecco's modified Eagle Media plus high glucose (4.5 g/l) and L-glutamine (4 mM) (HyClone-GE Health Sciences) supplemented with 10% (v/v) fetal bovine serum (Gibco), 50 U/ml penicillin (Gibco), 50 μg/ml streptomycin (Gibco), 100 μg/ml normocin (Invivogen), 30 μg/ml blasticidin (Invivogen) and 100 μg/ml zeocin (Invivogen) under standard conditions of 37°C, 5% CO_2.

THP1-TLR9 cells were grown according to manufactures' instruction in a maintenance media of RPMI 1640 and L-glutamine (2 mM) (HyClone-GE Health Sciences) supplemented with 10% (v/v) fetal bovine serum (Gibco), 50 U/ml penicillin (Gibco), 50 μg/ml streptomycin (Gibco), 100 μg/ml normocin (Invivogen), under standard conditions of 37°C, 5% CO_2.

For PS-ASO immune response analyses, 293-TLR9 and THP1-293 cells were washed in PBS and resuspended in HEK-Blue detection solution at a final concentration of 5×10^4 cells/well in a 96-well plate with indicated PS-ASOs and proteins. After 16 h incubation at 37°C, the optical density (OD) of the samples was measured at a wavelength of 620 nm using a microplate reader.

Bjab cells were maintained in Roswell Park Memorial Institute (RPMI) 1640 Medium supplemented with 20% fetal bovine serum (FBS), 0.1 μg/ml streptomycin and 100 units/ml penicillin. Prior to treatment, Bjab cells were washed in RPMI medium and were placed in a v-bottom 96-well dish at 50 000 cells per well prior to indicated PS-ASO addition by free uptake. Following indicated treatment time, cells were pelleted, lysed and total RNA was prepared, and levels of RNAs were quantified using qRT-PCR. Briefly, TLR9-KO Bjab cells were generated via CRISPR/Cas9 gene disruption resulting in a 40bp deletion in the TLR9 gene (29).

Proteome profiler

The release of chemokines was assayed using a Proteome Profiler™ Antibody Human XL Chemokine Array Kit (#ARY017) from R&D Systems Inc. according to the manufacturer's instructions

Affinity selection

Affinity selection using indicated biotinylated PS-ASOs was performed as described previously (28). Isolated proteins were separated on SDS-PAGE and analyzed by silver staining.

SiRNA treatment

100 μl of 1×10^6 of Bjab cells and 1 μM of siRNA were added to a BTX high throughput electroporation plate. The cells were then electroporated at 130 V using an ECM 830 high throughput electroporation system. siRNAs were transfected at 10 nM final concentration in 293-TLR9 cells plated the prior day using Lipofectamine RNAiMAX (Life Technologies), according to the manufacturer's protocol. At 48 h after siRNA transfection, cells were reseeded for activity analysis.

PS-ASO uptake analysis

Bjab cells were incubated with Cy3-labeled PS-ASOs for 4 h in a 37°C incubator. Following treatment, Bjab cells were washed 3 times with $1\times$ PBS supplemented with 3% FBS, to remove residual medium and external PS-ASOs. Cells were resuspended in $1\times$ PBS supplemented with 3% FBS for analysis by flow cytometry using an Attune NxT Flow Cytometer (ThermoFisher Scientific). Controls were performed by incubating PS-ASOs with cells on ice to demonstrate that washing steps remove the vast majority of PS-ASOs that were not taken into the cells (data not shown).

NanoBRET binding assay

N-terminal NLuc fusions were created using the vector pFN31K Nluc CMV-neo (Promega). Briefly, coding sequences of proteins were amplified from plasmids (Origene) using PCR primers complementary to the full-length cDNAs (information listed in supplementary materials and methods). The PCR products were ligated to XhoI and EcoRI sites of the pFN31K Nluc CMV-neo vector, as described previously (30). Fusion proteins were expressed by transfecting the plasmid into 6×10^5 HEK 293 cells using Effectene transfection reagent (Qiagen) according to the manufacturer's protocol. Following a 24 h incubation, cells were removed from the plate by trypsinization, washed with

$1 \times$ PBS, and resuspended in 250 µl Pierce IP Lysis Buffer (Thermo Scientific). Lysates were incubated 30 min at 4°C while rotating, then debris was pelleted by centrifugation at 15 000 rpm for 5 min. The fusion protein was purified by adding 20 µl HisPur Ni-NTA Magnetic Beads (Thermo Scientific) and 10 mM imidazole then incubating at 4°C for 2 h. Beads were washed five times with $1 \times$ PBS, 10 mM imidazole and 0.01% Tween-20. Fusion protein was eluted from the beads in 100 µl $1\times$ PBS and 200 mM imidazole, followed by dilution with of 200 µl IP buffer.

BRET assays were performed in white 96-well plates as previously described (31). Alexa 594-linked PS-ASO 1024788 as well as indicated PS-ASOs were incubated at room temperature for 15 min in $1 \times$ binding buffer (100 mM NaCl, 20 mM Tris–HCl, pH 7.5, 1 mM EDTA and 0.1% NP-40) with 10^6 RLU/well of Ni-NTA-purified NLuc fusion protein. Following the incubation, NanoGlo substrate (Promega) was added at 0.1 µl/well. Readings were performed for 0.3 s using a Glomax Discover system using 450/8 nm band pass for the donor filter, and 600 nm long pass for the acceptor filter. BRET was calculated as the ratio of the emission at 600/450 nm (fluorescent excitation emission/RLU).

RESULTS

Non-CpG PS-ASOs elicit innate immune responses via the TLR9 pathway

We first utilized Bjab cells to determine the cellular pathways responsible for the innate immune responses to non-CpG PS-ASOs. The Bjab cell line has been recently validated as a means of predicting PS-ASO immune activation in patients and as a model for studying PS-ASO TLR9-dependent innate immune activation *in vitro* (23,29). Throughout this study, we used several PS-ASOs that elicited strong innate immune responses in comparison to other PS-ASOs such as PS-ASO-38 that does not appear to significantly activate the innate immune system (29). This series of PS-ASOs includes a variety of PS-ASO designs, including full PS and PS/PO mixed backbone and $2'$ MOE modified ASO sequences as well as 3–10-3 cEt PS-ASOs of various sequences (Figure 1A). The transcriptional indicator of innate immune activation used for this assay (29), CCL22 mRNA, increased significantly, as compared with mock treatment (UTC) (Figure 1B). The upregulation was essentially fully abrogated in TLR9 KO cells (Figure 1B), consistent with previous results for other PS-ASOs (19). Furthermore, analysis of a panel of secreted immune markers revealed common indicators of TLR9 activation using the CpG PS-ASO; importantly, no alternative immune markers were upregulated with the non-CpG PS-ASO 95 (Supplementary Figure S1). As a negative control, no substantial upregulation of these immune markers was observed for PS-ASO 38. This further suggests that our model PS-ASOs utilize the TLR9 pathway of innate immune activation in the model systems utilized.

Next, we tested these PS-ASOs in an additional model system, HEK293 cells with TLR9 overexpressed (293-TLR9) and an engineered NF_KB reporter system. Here, we found that while PS-ASOs 04 and 20 showed innate immune responses (and the CpG PS-ASO, as expected), several other PS-ASOs that induced innate immune responses in the Bjab cells showed minimal activation in the 293-TLR9 cells, suggesting that factors beyond TLR9 play important roles in innate immune cellular responses (Figure 1C and D). Subsequent experiments using the 293-TLR9 cells were therefore only tested with these three PS-ASOs.

We note that PS-ASO 04 contains 5 Thymines in a row, a motif shown to be immunogenic (32). However, other PS-ASOs with T-tracts investigated in pre-clinical screening were not shown to be immunogenic (data not shown), suggesting that other features in this sequence contribute to its immunogenicity.

Disruption of the TLR9 signaling pathway leads to reduced non-CpG PS-ASO immune responses

We utilized siRNAs to reduce UNC93B1 and MyD88, both proteins that are necessary for TLR9 signaling (Figure 2A–D (some data are spilt between two panels)). The reduced innate immune activation observed further confirms the involvement of the TLR9 pathway (9). Next, we observed that Chloroquine, which disrupts TLR9 signaling by altering endosomal integrity (33), decreased PS-ASO innate immune responses in both cell model systems (Figure 2E G (some data are spilt between two panels)). Overall, these data (Figures 1 and 2) suggest that non-CpG PS-ASOs require the canonical TLR9–MyD88–NF_KB pathway to generate innate immune responses, similarly to CpG PS-ASOs.

Intracellular trafficking proteins regulate PS-ASO immune responses

PS-ASO innate immune responses require PS-ASO-TLR9 binding interactions to occur in late endosomes (LEs). Inactive TLR9 resides in the ER and travels through the Golgi to end up in endocytic vesicles (9). PS-ASOs enter cells through the endocytic pathway and are eventually released mostly from LEs to the cytosol and nucleus where they are functional (34). It has been recently established that several proteins associated with ER-Golgi transport, such as COPII protein Sec31a and Golgi protein syntaxin-5, relocalize to PS-ASO-containing LEs, and both are needed for optimal PS-ASO antisense activity (30,34). For example, COPII vesicles were shown to relocate to LEs in the presence of PS-ASOs and inhibiting that process reduced PS-ASO activities (30). Here, we demonstrated that siRNA-mediated reduction of Sec23a and Sec31a, COPII coat proteins, reduced PS-ASO innate immune responses (Supplementary Figure S2A and B) in 293-TLR9 cells. This result was expected as TLR9 requires COPII vesicles for its trafficking. Interestingly, however, reduction of Syntaxin-5 and Syntaxin-6, proteins involved in tethering and fusion of vesicles to the Golgi, resulted in enhanced innate immune responses (Supplementary Figure S2C and D). On the other hand, reduction of Syntaxin 5 decreases PS-ASO activity (30,34). Recent studies identifying cellular factors that act to limit TLR9 activation by preventing its trafficking suggest that Syntax-5 and Syntaxin-6 perform a similar role (17,18). Clearly, the factors that regulate PS-ASO antisense activity are different than those that regulate PS-ASO innate immune response. In addition, our data suggest that there are novel proteins that block TLR9 trafficking.
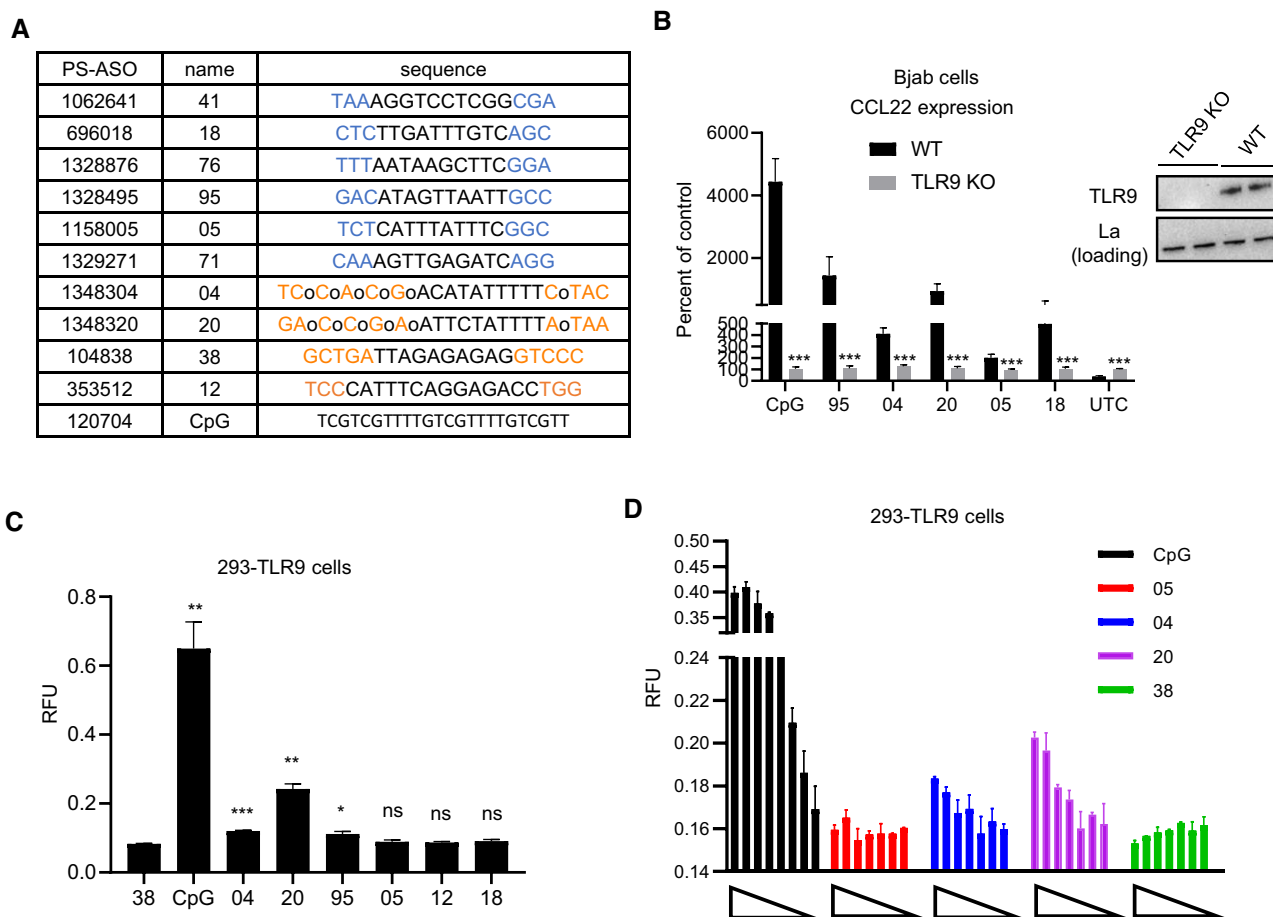
A

PS-ASO	name	sequence
1062641	41	TAAAGGTCCTCGGCGA
696018	18	CTCTTGATTTGTCAGC
1328876	76	TTTAATAAGCTTCGGA
1328495	95	GACATAGTTAATTGCC
1158005	05	TCTCATTTATTTCGGC
1329271	71	CAAAGTTGAGATCAGG
1348304	04	TCoCoAoCoGoACATATTTTTCoTAC
1348320	20	GAoCoCoGoAoATTCTATTTTAoTAA
104838	38	GCTGATTAGAGAGAGGTCCC
353512	12	TCCCATTTCAGGAGACCTGG
120704	CpG	TCGTCGTTTTGTCGTTTTGTCGTT

B

C

D

Figure 1. Non-CpG PS-ASOs generate immune responses via the TLR9 pathway. (**A**) Model PS-ASOs. 'o' corresponds to phosphodiester linkage; all other linkages are phosphorothioate. Blue and orange indicate cEt and MOE 2′ modifications respectively. (**B**) Relative qRT-PCR levels of *CCL22* mRNA in WT or TLR9-KO Bjab cells following 8 h incubation of indicated PS-ASOs at 1.6 μM in serum-free RPMI media by free-uptake. (right) Western blot analysis of TLR9 from indicated cells. (**C**) Relative fluorescence units (RFU) representing alkaline phosphatase activity under the NFKB promotor of HEK293 cells expressing hTLR9 (293-TLR9) showing TLR9 activation from 10 μM of the indicated PS-ASOs for 16 h. (**D**) RFU of TLR9 activation for 16 h with the indicated PS-ASOs in the following descending concentrations in μM: 10, 5, 2.5, 1.25, 0.62, 0.31, 0.156. Error bars are standard deviations from at least three independent experiments. P-values were calculated based on unpaired t-test and were computed comparing with control (WT or Luciferase) samples. ***$P < 0.001$; **$P < 0.01$; *$P < 0.05$; ns, not significant.

Previous reports have demonstrated the role of DNASE2-dependent ASO digestion to generate ASO fragments that can activate TLR9 ([16]). However, we show here that DNASE2 reduction does not alter PS-ASO immune responses in 293-TLR9 cells (Supplementary Figure S2E), likely due to the extent of the PS content of our PS-ASOs and the 2′modifications that enhance nuclease resistance.

PS-ASOs display different kinetics of innate immune activation yet bind to TLR9 with similar overall affinities

We observed that PS-ASOs display differential kinetics of innate immune stimulation, even though these PS-ASOs may have similar levels of immune activation at a later time (Figure 3A and B). For example, the CpG PS-ASO generates a significant innate immune response within 2 h, while the other PS-ASOs displayed no responses at that time point. In addition, some PS-ASOs showed responses at 4 h while responses to others were even more delayed. We hypothesized that this phenomenon could be due to either differences in signaling downstream of TLR9 (i), upstream of TLR9 (ii), or due to different interactions at the PS-ASO-TLR9 interface (iii). Here, we address these three possibilities: (i) First, we found protein phosphorylation markers of innate immune activation (Figure 3C) display similar kinetic trends to those from mRNA transcriptional analyses (Figure 3A). This suggests that the kinetic discrepancies are unlikely to be manifested from interactions downstream of TLR9. (ii) To determine if there is a correlation between PS-ASO innate immune kinetics and overall cellular PS-ASO uptake, we monitored cellular levels of Cy3-labeled versions of our PS-ASOs using flow cytometry and the results suggest that PS-ASO uptake is not a determining factor for the different kinetics of innate immune activation (Figure 3D). For example, 'slow' PS-ASO 05 is taken by the cells more readily than 'faster' PS-ASOs 95 or 04.

iii) Next, we performed PS-ASO-TLR9 binding analyses using the NanoBret assay ([31]) (Figure 3E and F). Here, indicated PS-ASOs were mixed with a fixed concentration
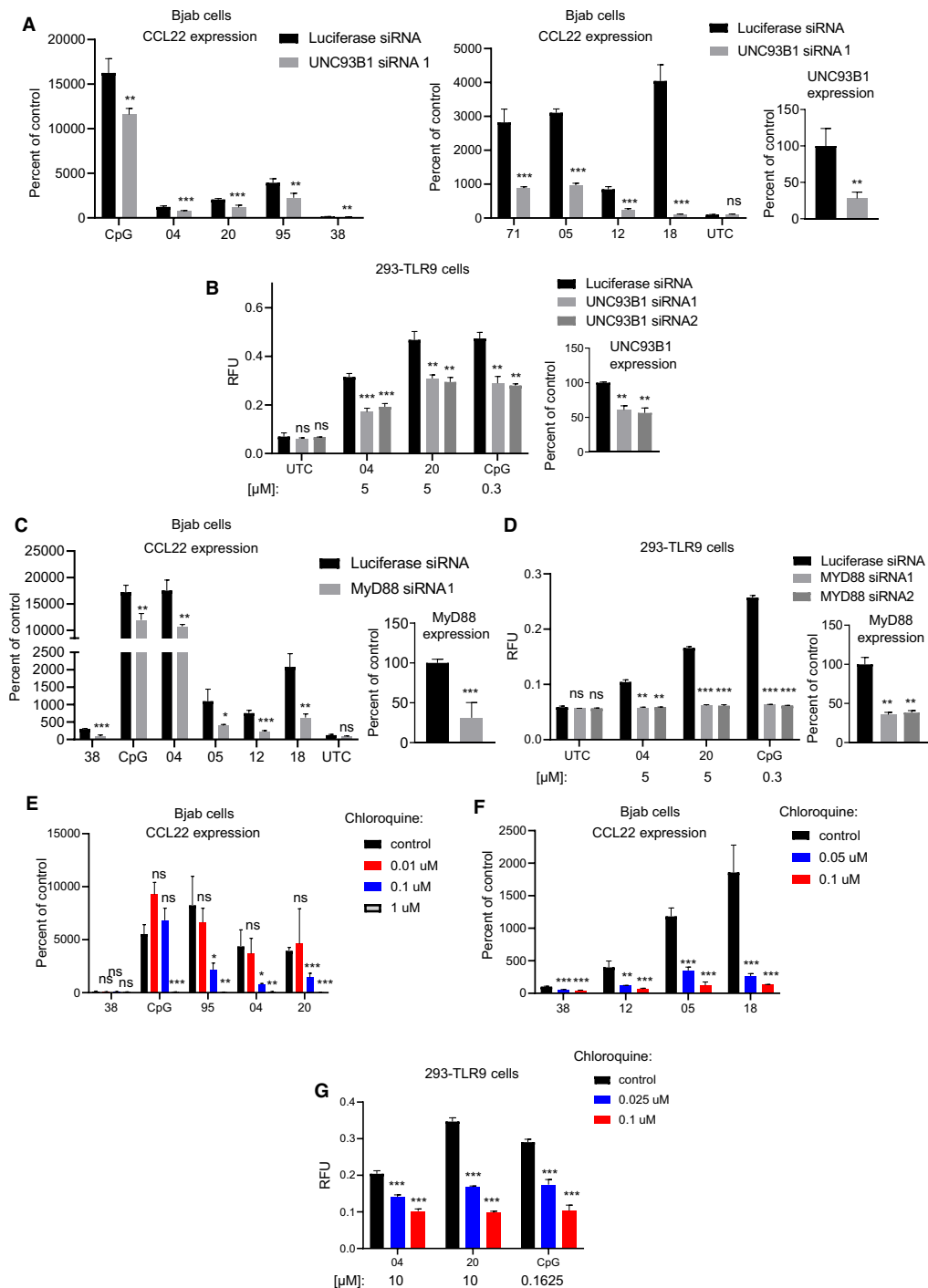
Figure 2. Disruption of the TLR9 signaling pathway leads to reduced immune responses for non-CpG PS-ASOs. (**A**) Relative qRT-PCR levels of *CCL22* mRNA in either control Luciferase or UNC93B1-targeted siRNA treated Bjab cells following incubation of indicated PS-ASOs at 1.6 μM in serum-free RPMI media by free-uptake for 8 h (left) or 4 h (middle). Relative qRT-PCR levels of *UNC93B1* mRNA for indicated Bjab cells shown to the right. (**B**) RFU of TLR9 activation for either control Luciferase or UNC93B-targeted siRNA in 293-TLR9 cells treated with the indicated PS-ASOs for 16 h. Relative qRT-PCR levels of *UNC93B* mRNA for indicated 293-TLR9 cells shown to the right. (**C**) Relative qRT-PCR levels of *CCL22* mRNA in either control Luciferase or *MyD88*-targeted siRNA Bjab cells following 16 h incubation of indicated PS-ASOs at 1.6 μM in serum-free RPMI media by free-uptake. Relative qRT-PCR levels of *MyD88* mRNA for indicated Bjab cells shown to the right. (**D**) RFU of TLR9 activation for either control Luciferase or MyD88-targeted siRNA in 293-TLR9 cells treated with the indicated PS-ASOs for 16 h. Relative qRT-PCR levels of *MyD88* mRNA for indicated 293-TLR9 cells shown to the right. (**E**) Relative qRT-PCR levels of *CCL22* mRNA in Bjab cells following 8 h incubation with the indicated PS-ASOs at 1.6 μM in serum-free RPMI media by free-uptake with the indicated amount of Chloroquine added. (**F**) Relative qRT-PCR levels of *CCL22* mRNA in Bjab cells following 16 h incubation with the indicated PS-ASOs at 1.6 μM in serum-free RPMI media by free-uptake with the indicated amount of Chloroquine added. (**G**) RFU of TLR9 activation for 293-TLR9 cells treated with the indicated PS-ASOs incubated with the indicated amount of chloroquine for 16 h. Error bars are standard deviations from at least three independent experiments. P-values were calculated based on unpaired *t*-test and were computed comparing with control (WT or Luciferase) samples. ***$P < 0.001$; **$P < 0.01$; *$P < 0.05$; ns, not significant.
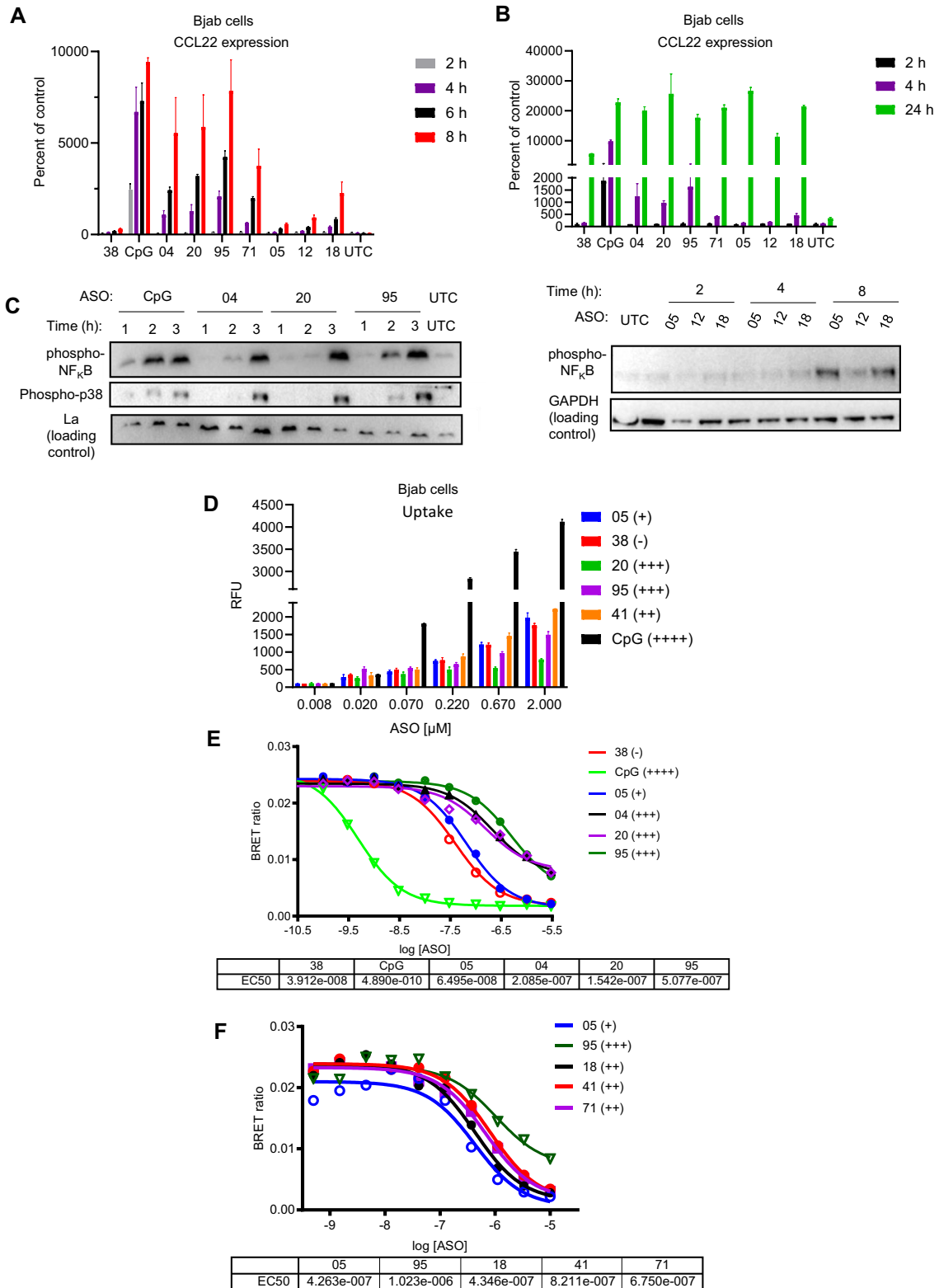
Figure 3. PS-ASOs display different kinetics of immune activation (**A** and **B**) Relative qRT-PCR levels of *CCL22* mRNA in Bjab cells following incubation of indicated PS-ASOs at 1.6 μM in serum-free RPMI media by free-uptake at the indicated time points. (**C**) Western blot analysis of indicated proteins at indicated time points in Bjab cells following incubation of 1.6 μM of indicated PS-ASOs. La and GAPDH were probed and used as loading controls as indicated. (**D**) Flow cytometry analysis of indicated Cy3-labeled PS-ASO uptake in Bjab cells following 4 h incubation. 'plus' signs indicate relative immune kinetics via (A). (**E** and **F**) NanoBRET assay for binding of indicated PS-ASOs with TLR9. The relative binding *kd*s (M) were determined via Graphpad prism and are present under the curves. Error bars are standard deviations from three independent experiments.

of Alexa 594-linked PS-ASO 1024788 along with purified TLR9. Decreases in signal correspond to indicated PS-ASOs competing with the Alexa-PS-ASO for TLR9 occupancy. This can be used to compare relative binding affinities of our model PS-ASOs for TLR9. This was used to determine if relative tighter binding affinities were correlated with faster kinetics. Interestingly, this was not the case, as a lack of correlation between PS-ASO-TLR9 binding and PS-ASO innate immune activation kinetics was observed (Figure 3E and F). For example, 'fast-responders' PS-ASO 95 and PS-ASO 04 have weaker TLR9 binding in comparison to 'slow-responder' PS-ASO 05 (however, as it has been shown that protein binding can increase with longer PS-ASOs and higher PS numbers (28,35), the tight binding of the CpG PS-ASO is most likely attributed to the extent of its phosphorothioate content due to its larger size (22 nt), and not to its CpG content (see below)). In addition, direct comparison of several 3–10–3 cEt PS-ASO-TLR9 relative binding properties further highlights a lack of correlation between binding affinity and innate immune activation (Figure 3F). One limitation of this approach is that it is unknown if ASO 1024788 binds to all known TLR9-ASO binding sites, yet it appears to bind to the CpG site. Since none of our 3 potential hypotheses explain the observed kinetics phenomenon, we therefore, next sought to further probe the interactions of various PS-ASOs and TLR9 in cells to gain more insight into this complex system.

Combinations of PS-ASOs either compete for TLR9 occupancy or act cooperatively on TLR9

To determine if PS-ASOs display different kinetics of innate immune activation due to differential interactions between individual PS-ASOs and TLR9 in cells, we designed a competition experiment by co-incubating innate immune-stimulatory PS-ASOs with a PS-ASO that does not activate the innate immune system, PS-ASO 38 (Figure 4A). Here, we discovered that the addition of the non-innate immune stimulatory competition PS-ASO dramatically reduces the innate immune responses for several PS-ASOs, suggesting that the ability to contact TLR9 is not correlated to PS-ASO- innate immune activation. Importantly, this corroborates our data with the NanoBret assay (Figure 3E and F), showing a lack of correlation with TLR9 binding and TLR9 activation. Next, we designed a series of competition experiments where we took advantage of PS-ASO modifications that can alter innate immune function without changing PS-ASO sequence or length. For example, PS-ASO 71 is much more innate immune-stimulatory than a modified version of the PS-ASO with two PO bonds at the gap-wing junction (Figure 4B). Interestingly, these two ASOs appear to compete for TLR9 binding similarly, since adding them together at an equal ratio generates an innate immune response that is significantly less than the innate immune response of the parental PS-ASO version alone (Figure 4B). Further, the PO version added in increasing amounts correspondingly decreases the innate immune response. This outcome was essentially replicated using several other innate immune stimulatory 3–10–3 cEt PS-ASOs by competing with versions of the corresponding PS-ASOs that include

PO linkages (Supplementary Figure S3A-E). This data also corroborates that overall TLR9–PS-ASO interactions cannot be correlated with TLR9 activation. Finally, we note that the TLR9 competitive-antagonist ability of the PO-substituted PS-ASOs suggests that these ASOs are not losing immunogenicity simply because they are being degraded by nucleases.

Next, we performed another series of PS-ASO combination experiments (Figure 4C). Interestingly, we find that certain 3–10–3 cEt PS-ASOs cause a dramatic increase in innate immune response in combination with this PS-ASO. The PS-ASOs 05 and 18 that cause dramatic increases when in combination with PS-ASO 95 in Bjab cells also do so in the 293-TLR9 cells (Figure 4D). These data may be explained by the possibility that these PS-ASOs may work cooperatively by interacting at different sites on TLR9, leading to TLR9 activation.

Overall, while further experiments are required to fully understand these processes, our data suggest that different PS-ASOs may interact with different binding sites on TLR9, where PS-ASOs either compete for one site or can act cooperatively by binding to different sites on TLR9; importantly, both of these scenarios have been described previously (14,36,37). Finally, as a control, we monitored Cy3-labeled PS-ASO uptake with or without the same amount of unlabeled PS-ASO (Supplementary Figure S3F and G) or unlabeled PS-ASO with a different sequence (Supplementary Figure S3H). We found that the addition of the unlabeled PS-ASOs has essentially no effect on Cy3-labeled PS-ASO uptake up to 2 μM. However, at 20 μM, a decrease in uptake is observed suggesting saturation of this process (Supplementary Figure S3F). These controls suggest that the altered immune response by the addition of other PS-ASOs at this concentration is unlikely caused by altered total level of uptake of the innate immune stimulatory PS-ASOs.

Together, our data suggest that differential PS-ASO innate immune kinetics cannot be explained by PS-ASO uptake or differences in the major steps in the TLR9 signaling pathway. While overall PS-ASO-TLR9 binding affinities cannot be correlated with innate immune responses either, a potential explanation of this different kinetics is that PS-ASOs can act as full or partial agonists, where the higher immune responses correlate with stronger agonist properties, which we speculate may be correlated with the exact positioning of the PS-ASO on TLR9. The details of these innate immunogenic non-CpG PS-ASO-TLR9 interactions will require substantial effort to fully understand.

Differential innate immune responses depend on the number and position of CpG motifs but do not correlate with overall PS-ASO–TLR9 binding affinities

To contextualize the results of our analyses of non-CpG PS-ASOs, we next applied a similar set of experiments to unmethylated CpG containing PS-ASOs. We tested a series of PS-ASOs in which one to four CpG sites were mutated to non-immunogenic GpG sites within the canonical CpG-B PS-ASO (Figure 5A). (The CpG-B PS-ASO is a B-class PS-ASO, which stimulates B cells and signals via $NF_K B$ (38).) Several of these PS-ASOs with reduced num-
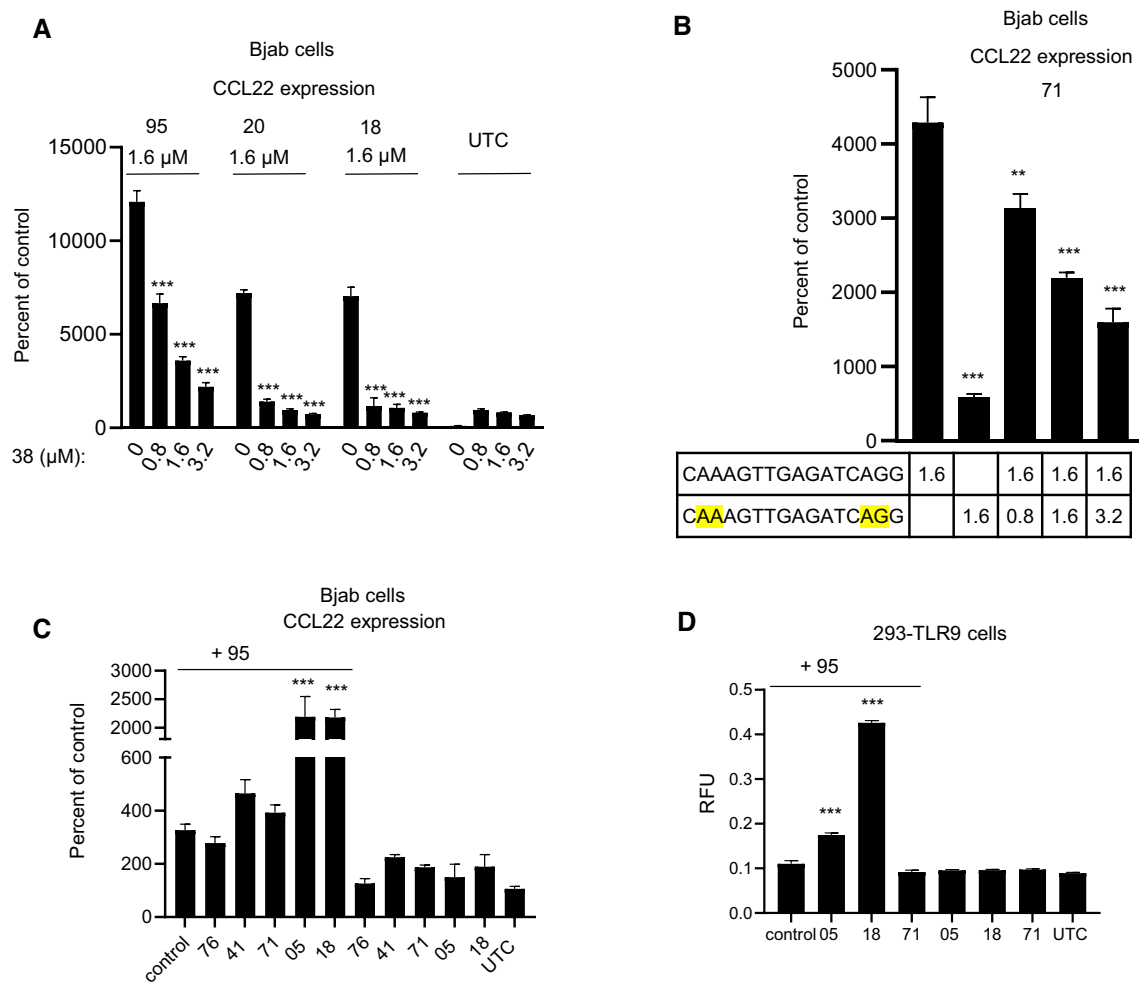
Figure 4. Combinations of PS-ASOs can either be competitive or cooperative for TLR9 activation (**A**) Relative qRT-PCR levels of *CCL22* mRNA in Bjab cells following co-incubation of indicated PS-ASOs at 1.6 µM in serum-free RPMI media by free-uptake for 8 h. Samples below the horizontal lines indicate co-incubated samples. (**B**) Relative qRT-PCR levels of *CCL22* mRNA in Bjab cells following co-incubation of indicated PS-ASOs at indicated concentrations in serum-free RPMI media by free-uptake for 8 h. Yellow highlighted nucleotides indicate PO bonds. (**C**) Relative qRT-PCR levels of *CCL22* mRNA in Bjab cells following co-incubation of 1.6 µM of indicated PS-ASOs in serum-free RPMI media by free-uptake for 3 h. Samples below the horizontal line indicates co-incubated samples. (**D**) RFU of TLR9 activation for 293-TLR9 cells treated with 5 µM of indicated PS-ASOs for 16 h. Samples below the horizontal line indicates co-incubated samples. Error bars are standard deviations from three independent experiments. P-values were calculated based on unpaired *t*-test and were computed comparing with control samples. ***$P < 0.001$; **$P < 0.01$; *$P < 0.05$; ns, not significant.

bers of the CpG motifs resulted in decreased innate immune activation in the 293-TLR9 cells, yet many still appeared to be capable of activation of innate immunity that was almost equal to the parent CpG sequence in the Bjab cells (Figure 5B and C). Further analysis of different time points showed several PS-ASOs containing one CpG motif exhibited delayed responses and the more 3' the CpG dinucleotide the more delayed response (Figure 5D). Interestingly, these 'slow-responders' resulted in limited activation in the 293-TLR9 cells. We note that slow response in Bjab cells and a lack of activity in the 293-TLR9 cells was also observed for the 'slow-responders' in the prior series of experiments (Figures 1C and 3A). The PS-ASOs with 2 or more CpG motifs tended to have stronger innate immune activation in both 293-TLR9 and Bjab cells, as has been shown previously (39). The levels of PS-ASO cellular uptake are comparable for these PS-ASOs (Figure 5E), suggesting that the altered innate immune response was not a

result of altered PS-ASO uptake. Also, we determined that non-immunogenic PS-ASOs can compete with the CpG-B PS-ASO for innate immune activation in both model systems (Figure 5F and G). Importantly, these experiments are in line with previous work (36,40). Although the number and position of the CpG motif are important for PS-ASO innate immune response, these two characteristics appear to not affect PS-ASO–TLR9 binding as determined via the NanoBret assay, used as described above where the indicated PS-ASOs compete for TLR9 occupancy with an Alexa-labeled PS-ASO (Figure 5H).

The data (Figures 3–5) are consistent with the explanation that PS-ASOs (both CpG and non-CpG) traffic to and bind to TLR9 yet display dramatically varied abilities to activate TLR9. We speculate that subtle differences between where and how they interact with TLR9 may explain their propensity for TLR9 activation, and studies are ongoing to develop a better understanding of these systems.
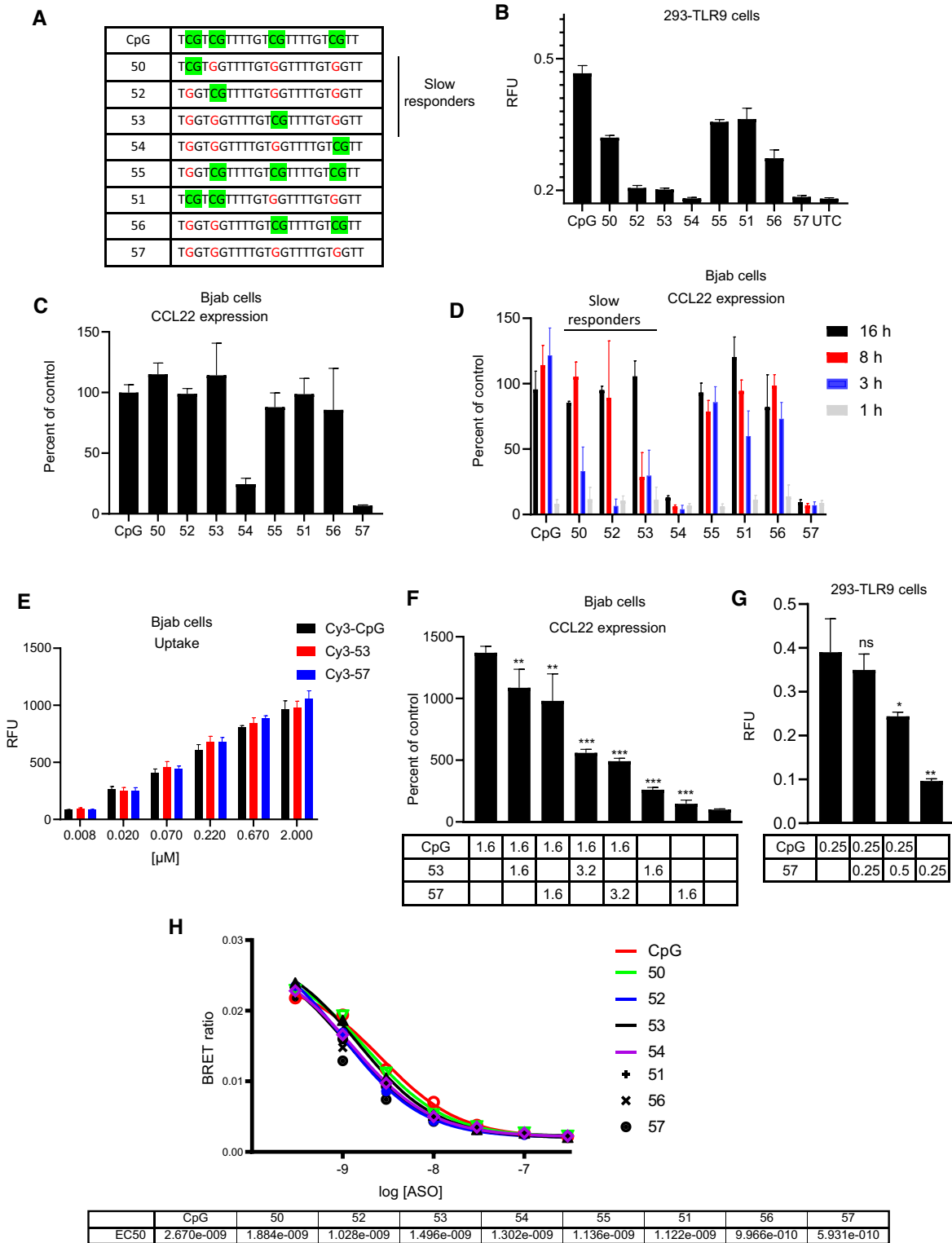
Figure 5. CpG number and position affect immune activation kinetics but not TLR9 occupancy. (**A**) Sequences of PS-ASOs with CpG sites highlighted in green. (**B**) RFU of TLR9 activation for 293-TLR9 cells treated with the indicated PS-ASOs for 16 h. (**C** and **D**) Relative qRT-PCR levels of *CCL22* mRNA in Bjab cells following incubation with indicated PS-ASOs at 1.6 μM in serum-free RPMI media by free-uptake for 16 h (C) or at indicated times (D). (**E**) Flow cytometry analysis of indicated Cy3-labeled PS-ASO uptake in Bjab cells following 4 h incubation. (**F**) Relative qRT-PCR levels of *CCL22* mRNA in Bjab cells following co-incubation of indicated PS-ASOs at 1.6 μM in serum-free RPMI media by free-uptake for 2 h. (**G**) RFU of TLR9 activation for 293-TLR9 cells treated with the indicated PS-ASOs for 16 h. (**H**) NanoBRET assay for binding of indicated PS-ASOs with TLR9. The relative binding *kd*s (M) were determined via Graphpad prism and are present under the curves. Error bars are standard deviations from three independent experiments. P-values were calculated based on unpaired t-test and were computed comparing with control (CpG) samples. ***$P < 0.001$; **$P < 0.01$; *$P < 0.05$; ns, not significant.

The subsequent sections of the manuscript interrogate the role of extracellular proteins in modulating PS-ASO–TLR9 activation.

The extracellular milieu affects PS-ASO innate immune responses

PS-ASO–protein interactions can alter the fates of PS-ASO uptake, trafficking, and subcellular localization, and in turn, can affect PS-ASO activity and toxicity (7). Interactions between PS-ASOs and plasma proteins have been documented (27), and the effects of PS-ASO–protein interactions in TLR9 activation has also been described for some proteins. For example, HMGB1 and Granulin have been documented to interact with CpG PS-ASOs to enhance innate immune responses (24,25), while human serum albumin (HSA)–PS-ASO–TLR9 interactions lead to decreases in innate immune responses (41). Consistently, we found that reduction of HMGB1 and Granulin by siRNA in our two model cell systems decreased the innate immune response of the non-CpG PS-ASOs and we also confirm the co-localization of PS-ASOs with granulin in cells (Supplementary Figure S4).

We sought to develop a more comprehensive understanding of how PS-ASO–protein interactions can alter PS-ASO innate immune responses. First, we found that the addition of human serum dramatically dampens PS-ASO innate immune responses in both Bjab and 293-TLR9 cells (Figure 6A and B, Supplementary Figure S5A and B). Similar results were found using FBS (Supplementary Figure S5C). Mouse, Rabbit, and Monkey Sera also lowered PS-ASO innate immune responses to a similar extent in Bjab cells (Supplementary Figure S5D–F) (27). Next, we asked if proteins that may be secreted by cells contribute to PS-ASO innate immune responses. To do this, we performed an experiment using conditioned media from Bjab cells and found that conditioned medium increased PS-ASO induced innate immune responses (Figure 6C). Interestingly, the conditioned media didn't enhance the innate immune response of the CpG PS-ASO, suggesting that the CpG PS ASO didn't require interactions with extracellular proteins to be a full agonist of the innate immune system (Figure 6D). Finally, we monitored Cy3-labeled PS-ASO uptake in Bjab cells and found that uptake was not significantly hindered with the addition of serum; An exception was the CpG PS-ASO, the long PS-DNA ASO, which showed reduced uptake upon serum addition, though not to the extent that the serum inhibited innate immune responses (Figure 6E-H). These results together suggest that PS-ASO–protein interactions do not seem to deter PS-ASO uptake under these experimental conditions, rather that they likely alter PS-ASO–TLR9 activation. Overall, our results suggest that certain extracellular proteins enhance innate immune responses, while others, especially those present in serum, decrease them.

Specific PS-ASO–protein interactions affect PS-ASO immune responses

We sought to identify proteins that complex with PS-ASOs to boost innate immune responses. We hypothesized that decreases in innate immune responses when replacing PS

with PO backbones at the gap-wing junction (Figure 4B) were correlated with altering certain PS-ASO–protein binding properties. Therefore, we performed a PS-ASO affinity selection assay in which we eluted PS-ASO-binding proteins captured from various media with an innate immune stimulatory full PS-ASO or the same PS-ASO but with two POs at each gap-wing junction. While the majority of proteins eluted at similar levels between the two competing PS-ASOs, there were select bands that were more heavily enriched in the parent, full PS-ASO lane (Supplementary Figure S6). These bands were excised and the proteins were identified by Mass spectrometry (Alphalyse, data not shown). Three proteins were identified as potential candidates: Histidine-rich glycoprotein (HRG), S100A8 and Compliment factor H-related protein 1 (CFHR1). Importantly these three proteins have been shown to bind PS-ASOs (27) and have been implicated in innate immune responses (42,43), yet their roles in the context of PS-ASO–TLR9 engagement remain unexplored, to the best of our knowledge. We also chose to study HMGB1, whose role in PS-ASO|TLR9 interactions has been noted (26).

We incubated either HRG, HMGB1 or S100A8 recombinant proteins with several of our innate immune-stimulatory PS-ASOs to determine if they affected the PS-ASO innate immune responses in both model systems. Indeed, we find that the presence of these proteins enhances innate immune responses of the PS-ASOs in most cases (Figure 7, Supplementary Figure S7A). Interestingly, the combination of PS-ASO 04 with HRG showed no substantial enhancement; and the results were consistent across the two model systems. We also compared the TLR9-dependent innate immune-stimulatory effects of S100A8 with the related protein S100A9 (which also can bind PS-ASOs (27)) and found that S100A8 is more potent. Finally, we demonstrated siRNA-mediated knockdown of S100A8 in TLR9-overexpressing THP1 monocyte cells (a cell type with appreciable levels of S100A8 (44)) demonstrated reduced immune responses to PS-ASOs (Supplementary Figure S7B). Overall, we identified novel innate immune stimulatory proteins that can enhance PS-ASO innate immune responses.

Since serum severely dampens innate immune responses (Figure 6), we tested if HSA, the major protein in serum, blocked PS-ASO innate immune responses, as has been previously shown (41). Indeed, we find that our PS-ASOs show reduced innate immune responses with the addition of HSA in both model systems (Supplementary Figure S7 C and D).

Innate immune stimulatory proteins selectively bind PS-ASOs relative to PO backbone-substituted versions.

We hypothesized that PO substitutions at the PS-ASO gap-wing junction decreased innate immune responses due to their diminished binding to select innate immune-stimulatory proteins, based on data from Supplementary Figure S6. To test this, we performed the NanoBret competition binding assay (as described above) by comparing binding of 3–10–3 cEt full PS PS-ASOs with versions of the PS-ASO with either 2 or 4 total substituted PO linkages. We indeed found that the addition of the POs resulted in decreases in PS-ASO–protein interactions in a PO number-dependent manner (Figure 8A–C, Supplementary
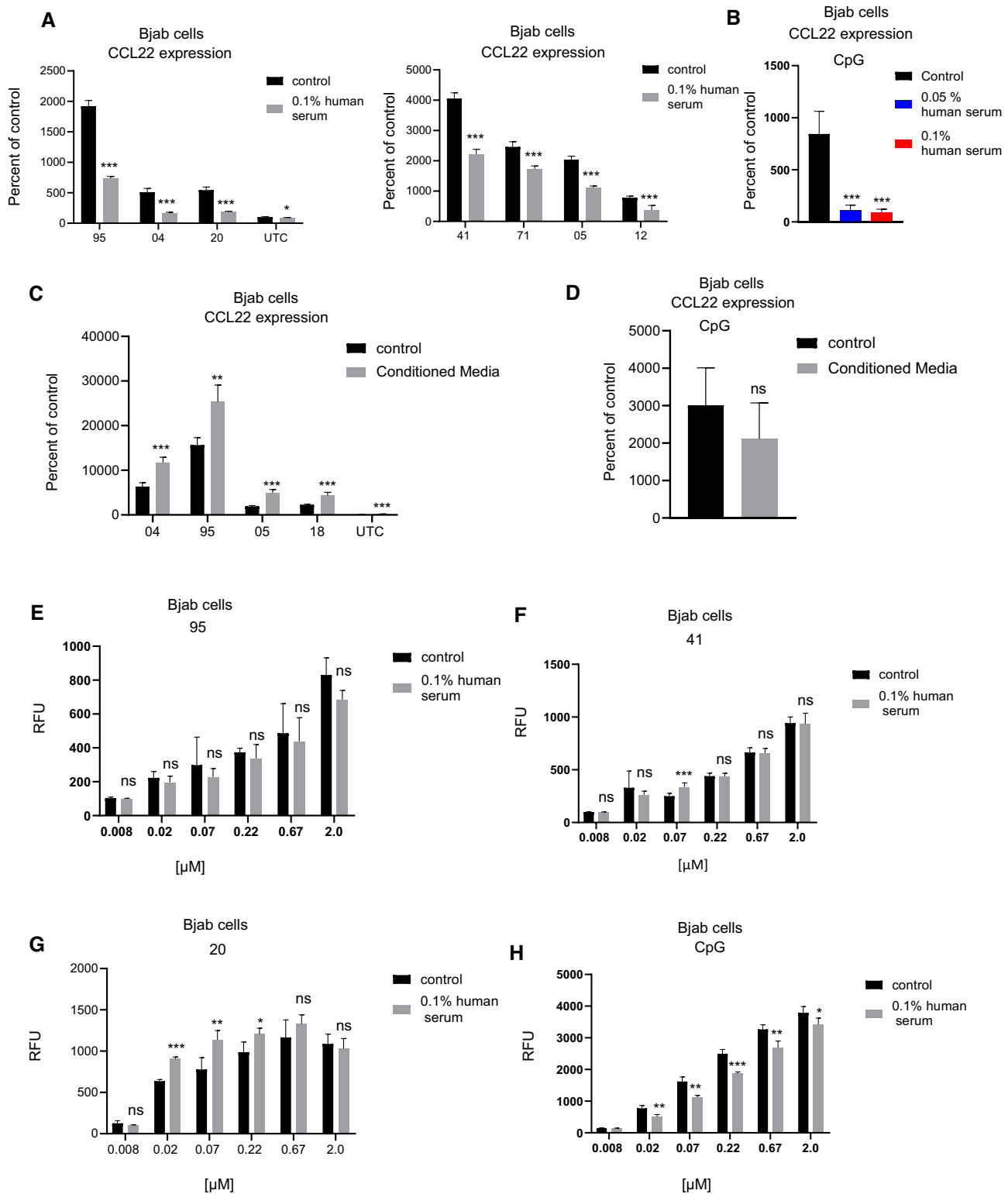
Figure 6. Extracellular milieu affects PS-ASO-immune responses. (**A**) Relative qRT-PCR levels of *CCL22* mRNA in Bjab cells following incubation with indicated PS-ASOs at 1.6 µM in serum-free RPMI media with indicated amounts of human serum added by free-uptake for 4 h (left panel) and 8 h (right panel). (**B**) Relative qRT-PCR levels of *CCL22* mRNA in Bjab cells following incubation with indicated PS-ASO at 1.6 µM in serum-free RPMI media by free-uptake for 2 h. (**C** and **D**) Relative qRT-PCR levels of *CCL22* mRNA in Bjab cells following incubation with indicated PS-ASOs at 1.6 µM in serum-free RPMI media or conditioned media by free-uptake for 8 h (C) or 2 h (D). Conditioned media was generated by incubating Bjab cells in serum-free RPMI media for 24 h. (**E-H**) Flow cytometry analysis of indicated Cy3-labeled PS-ASO uptake in Bjab cells following 4 h incubation. Error bars are standard deviations from three independent experiments. P-values were calculated based on unpaired t-test and were computed comparing with control samples. ***$P < 0.001$; **$P < 0.01$; *$P < 0.05$; ns, not significant.

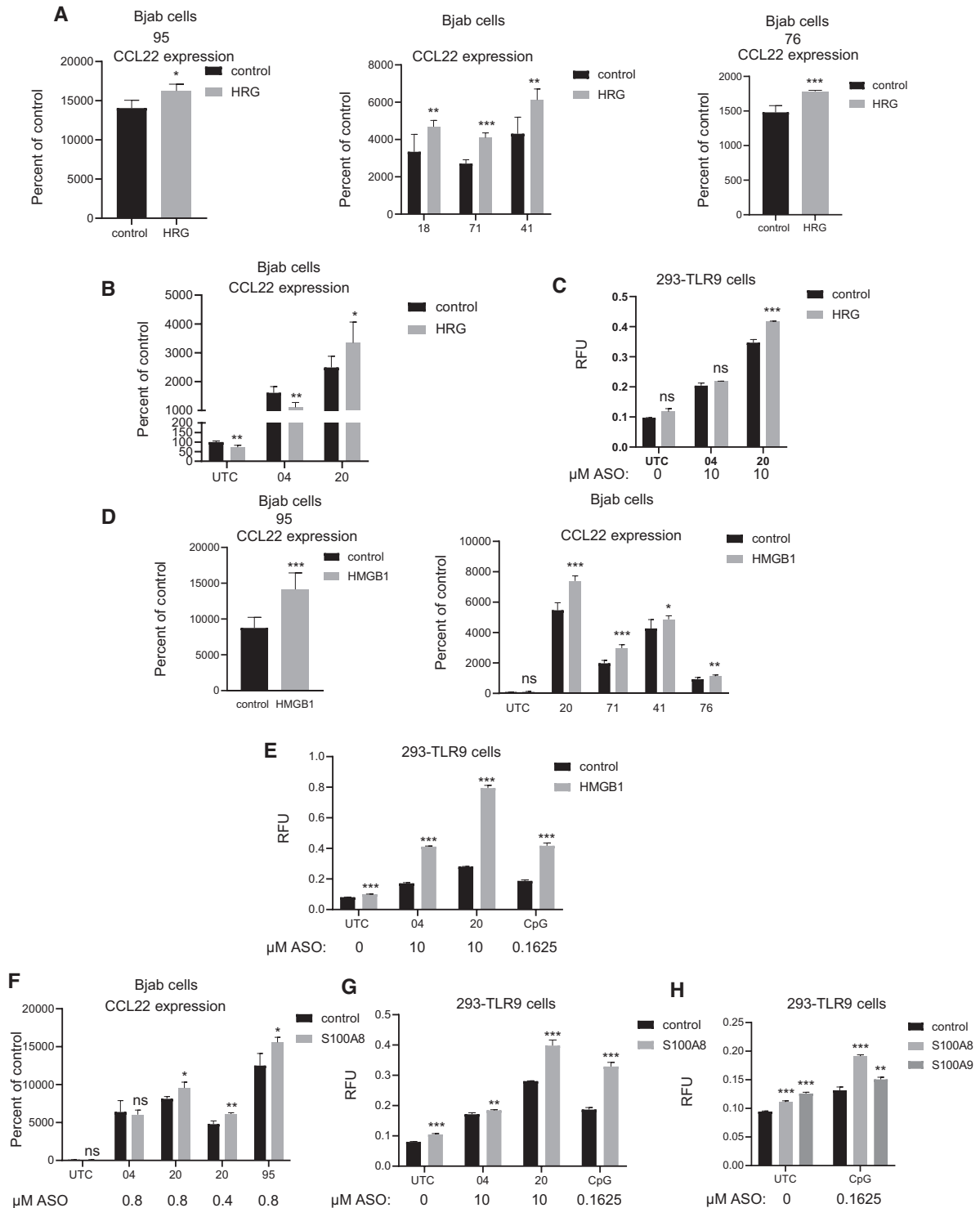**Figure 7.** Exogenous proteins affect PS-ASO-immune responses. (**A** and **B**) Relative qRT-PCR levels of *CCL22* mRNA in Bjab cells following incubation with indicated PS-ASOs at 1.6 μM in serum-free RPMI media without (black bars) or with (grey bars) 0.3 μM HRG at 7 h (A) or 4 h with indicated HRG concentrations (B). (**C**) RFU of TLR9 activation for 293-TLR9 cells treated with the indicated PS-ASOs for 16 without (black bars) or with (grey bars) 0.3 μM HRG. (**D**) Relative qRT-PCR levels of *CCL22* mRNA in Bjab cells following incubation with indicated PS-ASOs at 1.6 μM in serum-free RPMI media without (black bars) or with (grey bars) 0.5 μM HMGB1 for 8 h. (**E**) RFU of TLR9 activation for 293-TLR9 cells treated with the indicated PS-ASOs without (black bars) or with (grey bars) 0.5 μM HMGB1 for 16 h. (**F**) Relative qRT-PCR levels of *CCL22* mRNA in Bjab cells following incubation with indicated PS-ASOs in serum-free RPMI media without (black bars) or with (grey bars) 0.45 μM S100A8 for 7 h. (**G**) RFU of TLR9 activation for 293-TLR9 cells treated with the indicated PS-ASOs without (black bars) or with (grey bars) 0.45 μM S100A8 for 16 h. (**H**) RFU of TLR9 activation for 293-TLR9 cells treated with the indicated PS-ASOs for 16 h without (black bars) or with either 0.45 μM S100A8 or S100A9. Error bars are standard deviations from three independent experiments. P-values were calculated based on unpaired t-test and were computed comparing with control samples. ***$P < 0.001$; **$P < 0.01$; *$P < 0.05$; ns, not significant.
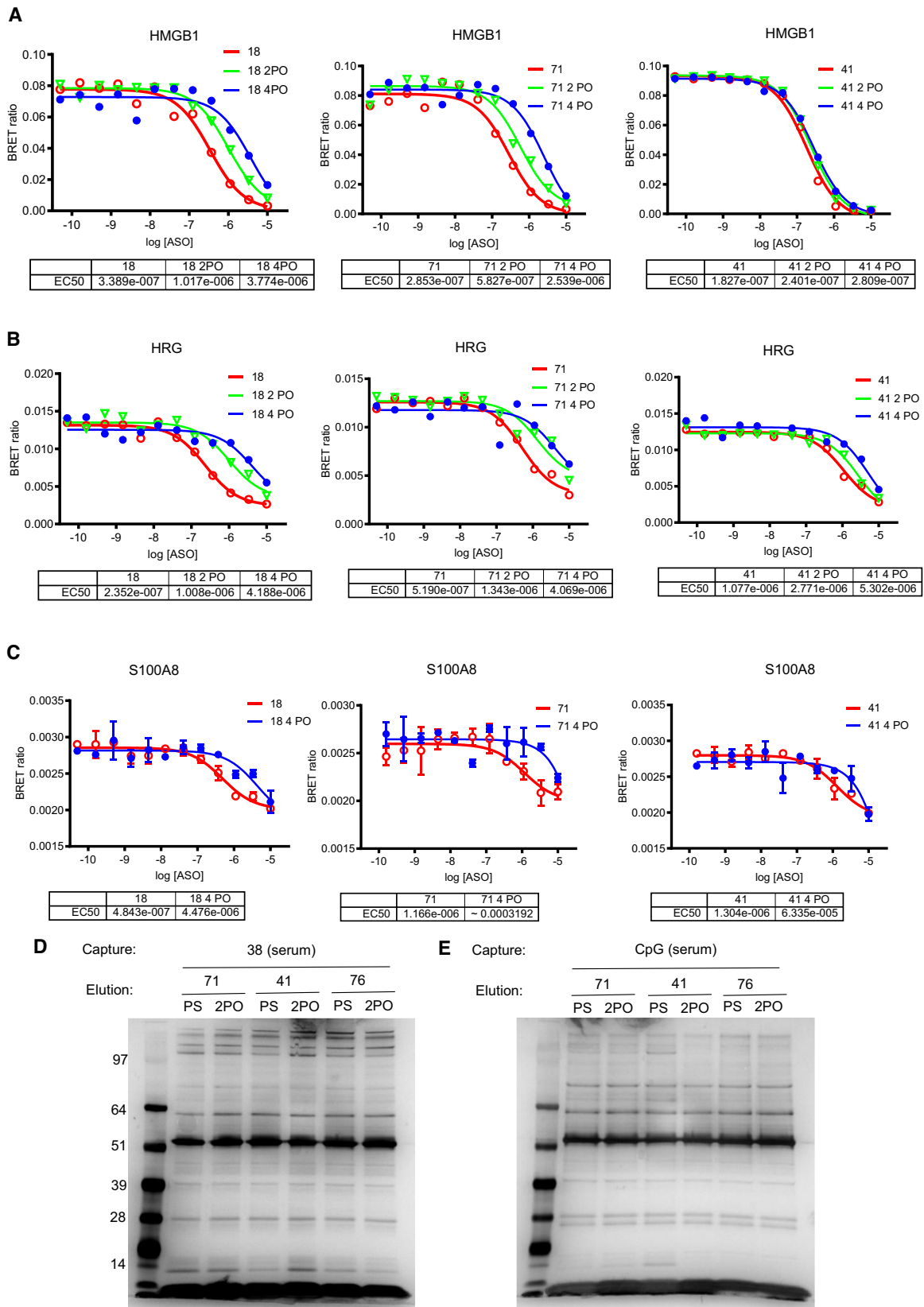
A

HMGB1

	18	18 2PO	18 4PO
EC50	3.389e-007	1.017e-006	3.774e-006

HMGB1

	71	71 2 PO	71 4 PO
EC50	2.853e-007	5.827e-007	2.539e-006

HMGB1

	41	41 2 PO	41 4 PO
EC50	1.827e-007	2.401e-007	2.809e-007

B

HRG

	18	18 2 PO	18 4 PO
EC50	2.352e-007	1.008e-006	4.188e-006

HRG

	71	71 2 PO	71 4 PO
EC50	5.190e-007	1.343e-006	4.069e-006

HRG

	41	41 2 PO	41 4 PO
EC50	1.077e-006	2.771e-006	5.302e-006

C

S100A8

	18	18 4 PO
EC50	4.843e-007	4.476e-006

S100A8

	71	71 4 PO
EC50	1.166e-006	~ 0.0003192

S100A8

	41	41 4 PO
EC50	1.304e-006	6.335e-005

D

E

Figure 8. PS-ASOs bind to immune-stimulatory proteins. (**A**–**C**) NanoBRET assay for binding of indicated PS-ASOs with HMGB1 (A), HRG (B) and S100A8 (C). The relative binding *kd*s were determined via Graphpad prism and are present under the curves. (**D** and **E**) PS-ASO-binding proteins were isolated from Human serum with 5′-biotinylated PS-ASOs, eluted by competition using 50 μM unconjugated PS-ASOs, separated on SDS-PAGE, and visualized via silver staining.

Figure S8A–C). Importantly, as a control, we determined that serum proteins captured by two different biotin-labeled PS-ASOs were similarly eluted by the PS and 2PO versions of the PS-ASOs, signifying that overall protein binding capacities are similar (Figure 8D and E). Overall, this data confirms that full PS-ASOs have a particular affinity for certain innate-immunogenic proteins. This data also suggests that the ability to bind to these proteins allows for the full PS-ASOs to be more innate immune-stimulatory than versions of the PS-ASOs with PO substituted backbones.

We next tested if non-CpG PS-ASO protein binding properties correlated with non-CpG PS-ASO immune activation kinetics. 'Faster' PS-ASOs did not bind tighter to either HMGB1 or HRG than 'slower' PS-ASOs (Supplementary Figure S8D and E). This suggests that these PS-ASO protein interactions cannot explain immune activation kinetics.

PS-ASOs and immunogenic proteins enter endo-lysosomes and co-localize at TLR9 activation complexes.

We next tested if these novel innate immune-stimulatory PS-ASO–protein complexes enter cells and are co-present in the endocytic organelles, as has been shown for other protein-CpG PS-ASO complexes (24). We added various Cy3-PS-ASOs with Alexa 647-labeled, purified proteins of interest, and administered lysotracker to perform live-cell imaging in Bjab cells. Indeed, we found that these proteins could co-localize with PS-ASOs in the endocytic organelles (Figure 9, Supplementary Figure S9). Furthermore, we demonstrate that immunosuppressive proteins also enter cells and co-localize with PS-ASOs by administering Alexa 647-HSA with various PS-ASOs, as has been previously shown (41) (Supplementary Figure S10). Next, we evaluated if these PS-ASOs and proteins were part of an activated TLR9 complex. Since we found that PS-ASO–TLR9 interactions were not necessarily correlated with TLR9 activation, we chose to see if the complex co-localized with MyD88, which is recruited to TLR9 upon its activation. As a proof of concept, we show that an innate immunogenic PS-ASO co-localized with MyD88 in both our Bjab and 293-TLR9 cell models, whereas the non-innate immune-stimulatory PS-ASO did not (Supplementary Figure S11). Finally, we incubated the PS-ASOs with the indicated proteins in Bjab cells and demonstrated that the PS-ASOs and proteins co-localize with MyD88, suggesting that these complexes exist within activated TLR9 complexes (Figure 10). Overall, our data indicate that these novel TLR9 regulatory proteins can interact with PS-ASOs extracellularly, are internalized as PS-ASO–protein complexes, interact with TLR9 and activate the TLR9 signaling process within cells.

DISCUSSION

In this study, we systematically evaluated the mechanisms of PS-ASO-induced innate immune responses by investigating selected model non-CpG PS-ASOs that were found to be uniquely innate immune-stimulatory. Internal trafficking pathways can also affect PS-ASO innate immune responses, and our results suggest novel proteins affecting TLR9 trafficking. Interestingly, certain non-innate immune stimula-

tory PS-ASOs can inhibit innate immune responses of pro-inflammatory PS-ASOs, likely through competition for interaction with TLR9. Alternatively, certain PS-ASOs can cooperatively enhance innate immune responses. SAR studies showed that for CpG PS-ASOs, the number and position of the CpG motif significantly affect the innate immune responses, whereas replacing particular PS backbone linkages with PO backbone linkages for non-CpG PS-ASOs can inhibit innate immune responses likely due to changes in select PS-ASO–protein interactions. We discovered that extracellular components contribute to the activation of PS-ASO innate immune responses, most likely through PS-ASO binding to certain proteins, such as S100A8, HMGB1, and HRG, which can co-internalize with PS-ASOs and contribute to the interaction of PS-ASOs with TLR9 in LEs, triggering downstream signaling pathways. Together, our study identified important steps involved in PS-ASO innate immune responses and proposes a potential mechanism (Figure 11), that can eventually facilitate the design of PS-ASOs to mitigate innate immune responses.

Immunogenic PS-ASOs rely on the TLR9 pathway

We found that PS-ASO innate immune responses depend on normal endocytosis pathways and are TLR9 dependent, which localizes to LEs when active. Further studies in animal models and other cell types, such as those involving TLR9-dependent IRF7 signaling (9), will need to be performed to investigate the role of TLR9 for our model non-CpG PS-ASOs. Canonical TLR9 signaling, which recruits the TLR responsive factor MyD88 to relay immunostimulatory signaling, appears to similarly act as the pathway for both CpG PS-ASOs, as well as non-CpG PS-ASOs with a variety of sequences and chemical modifications and results in NF_KB signaling and the production of various innate immune markers. We also observed that certain factors that regulate normal PS-ASO trafficking and endosomal release may have opposing outcomes when regulating PS-ASO innate immune responses. Given that recent reports suggest an elaborate mechanism of TLR9 regulation (to limit auto-immune responses) (17,18), it is plausible that Syntaxin 5 and 6 act to limit TLR9 trafficking, while also facilitating PS-ASO release from endosomes. Obviously, numerous proteins affect both PS-ASO and TLR9 trafficking and using PS-ASO innate immune responses as a readout may be of further use to understand the initial steps of PS-ASO uptake and trafficking.

Combinations of PS-ASOs can either compete for TLR9 binding or bind to different locations on TLR9

We determined that different PS-ASOs display different kinetics of innate immune activation, which has been observed by others (45). This phenomenon cannot be explained by differences in PS-ASO trafficking or overall PS-ASO-TLR9 binding parameters or PS-ASO–protein binding upstream of TLR9. Based on a series of competition experiments, we determined that inflammatory PS-ASOs can be blocked by PS-ASOs with modifications that render them inert with regard to innate immune activation. Furthermore, our experiments also suggest that PS-ASOs interact with different oligo recognition sites within TLR9,
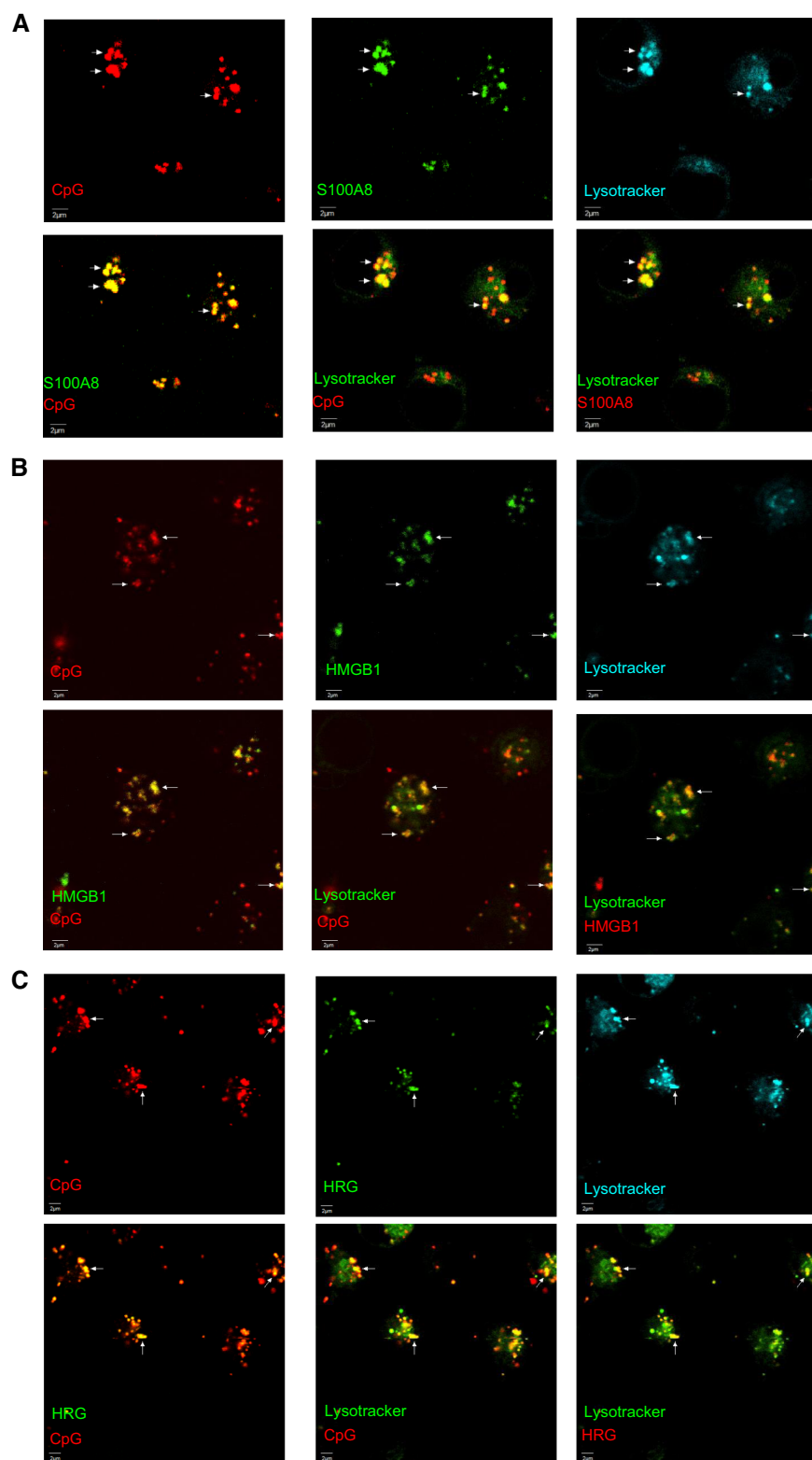
Figure 9. PS-ASO–protein complexes localize to endolysosomes. Live cell imaging of Bjab cells incubated with 2 μM of the indicated Cy3-PS-ASOs and 1 μM of the indicated Alexa 647-labeled protein for 2 h followed by addition of lysotracker for 0.5 h prior to imaging. Scale bars, 2 μm.
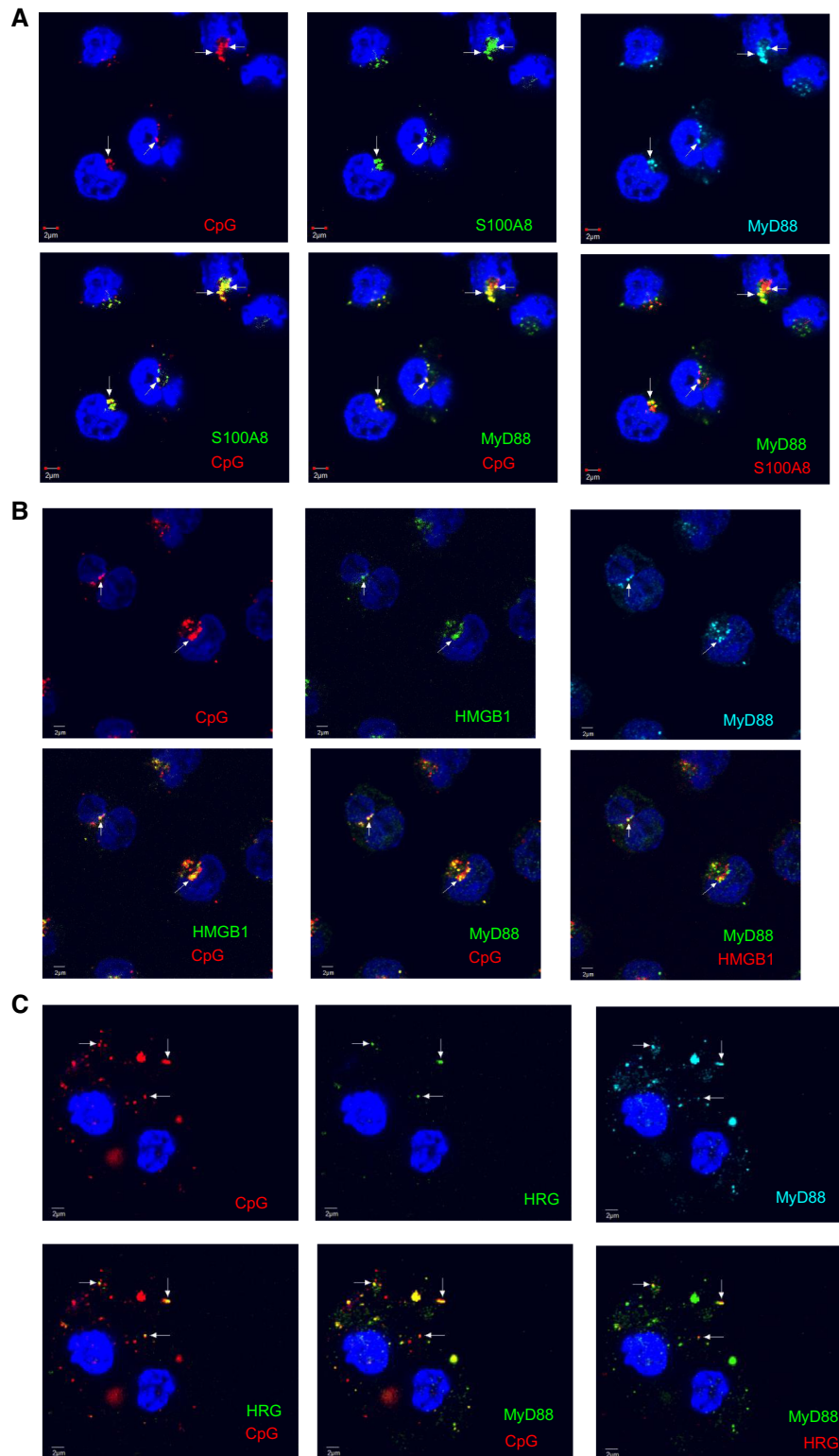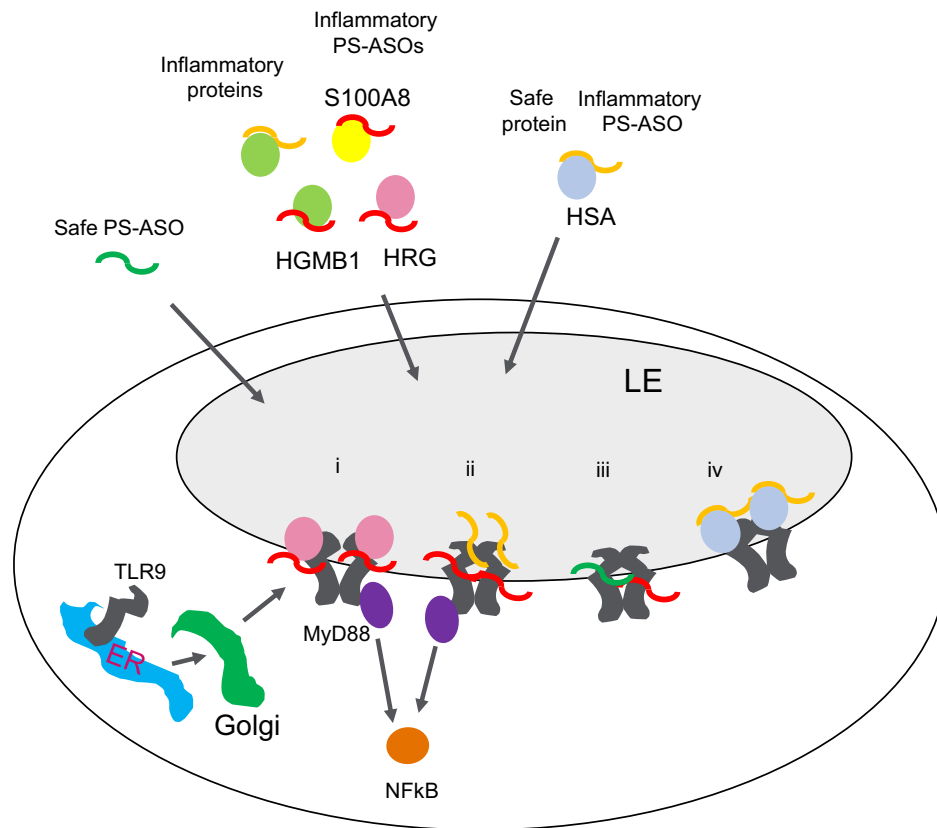
Figure 10. Immunogenic PS-ASO-Protein complexes co-localize with MyD88. Immunofluorescent staining of Myd88 in Bjab cells incubated with 2 μM of the indicated Cy-3 PS-ASOs and 1 μM of the indicated Alexa 647-labeled protein for 2 h. Scale bars, 2 μm.

Figure 11. Proposed model of various PS-ASO–protein–TLR9 interactions and consequences. (i) inflammatory PS-ASOs and inflammatory proteins interact with TLR9 to cause enhanced immune responses. (ii) Inflammatory PS-ASOs can synergistically enhance immune responses, likely by interacting at two different sites on TLR9. (iii) Non-innate immune stimulatory ('safe') PS-ASOs can block inflammatory PS-ASOs via competition for the same TLR9 binding site. (iv) Safe proteins can block PS-ASO–TLR9 immune activation.

as certain PS-ASO combinations can be cooperative while others are competitive. This notion is supported by recent reports showing that short, non-CpG oligos enhance CpG oligo innate immune responses by binding to an established alternative site on TLR9 (14,37), and a similar concept suggesting multiple nucleic acid binding sites on TLR7/8 has been demonstrated (32,46,47). Furthermore, inhibitory PS-ASOs were shown to partially overlap with immunogenic CpG PS-ASOs in a previous structural study (13), suggesting, overall, a broad range of potential PS-ASO-TLR9 configurations could exist that dictate TLR9 activation states. This suggests that PS-ASOs can act as partial agonists, where the positioning of the PS-ASOs on TLR9 governs the innate immune responses, which we are in the process of investigating further. This general concept of partial agonist-receptor interactions has been established in other systems (48,49).

PS-ASO-Protein interactions affect TLR9 signaling

The majority of the non-CpG PS-ASOs that show activity in Bjab cells, an established immune cell line that can be used to predict PS-ASO immune activation in patients (29), fail to show immune responses in the 293-TLR9 cells. This underscores the complexity of cellular innate immune activation. In addition, certain PS-ASOs can show responses in

the 293-TLR9 cells only when added with other PS-ASOs that can together induce cooperative TLR9 activation. This data suggests that the 293-TLR9 cells are sufficient to induce immune activation, yet they may lack certain factors that make TLR9 more responsive to non-canonical agonists, which we are in the process of trying to understand further.

PS-ASO–protein interactions play important roles in innate immune response, including extracellular components. Previous data demonstrated that HSA dampens TLR9 activation by blocking direct CpG PS-ASO access to TLR9 (41). Our experiments show that serum from various species dampens innate immune responses. Interestingly, conditioned medium enhances PS-ASO innate immune responses, as has been observed by others (27). It is likely that secreted proteins can interact with PS-ASOs to form certain PS-ASO–protein complexes to internalize together, place PS-ASOs in a competent conformation that interacts with TLR9 (50), and enables TLR9 activation and downstream signaling. Interestingly, these conformational changes have been shown to facilitate TLR9 activation in a PS-ASO-sequence independent manner (50).

Indeed, by affinity selection, we identified proteins from the extracellular medium that preferentially bind to immunostimulatory PS-ASOs. While these proteins have been

shown to bind PS-ASOs, their roles in PS-ASO-TLR9 activation were previously undetermined. We showed that the PS-ASO–protein complexes induce innate immune responses in both immune cells and a non-immune model (293-TLR9 cells); the latter highlights the TLR9-specific role of these effects as these proteins have been associated with other TLRs (43,51). Furthermore, we provided evidence of these PS-ASO–protein interactions within endocytic organelles and at TLR9-activated complexes. This general concept has already been established for other proteins complexing with CpG oligos (24), but here we extend this to include non-CpG PS-ASOs with various chemical modifications.

PO linkages limit immunogenic protein–PS-ASO interactions

We show that PS-ASOs where two of the 15 PS linkages are substituted with PO linkages, exhibit diminished innate immune responses, consistent with previous observations (22). This is likely due to alterations with specific innate immune-modulatory proteins. Importantly, however, this subtle backbone substitution does not affect overall protein binding properties, as also suggested by previous data (28). Yet further substitution with more PO linkages has been correlated with decreased overall protein binding (7,35). Further experiments will be required to exclude the role of nuclease-mediated ASO degradation in altering immune responses when replacing PS with a PO linkages; in addition, more analysis of the role of the PO linkages in the immunogenic properties of mixed backbone PS-ASOs 04 and 20 will need to be performed. Overall, our data suggest that extracellular protein–PS-ASO interactions likely dictate PS-ASO innate immune responses, as these proteins likely act as a frontline sensor and then rely on TLR9 to initiate the signal transduction.

PS-ASO drugs are commonly used and have enormous potential to treat various diseases. Some PS-ASO sequences can induce innate immune responses which can be avoided by *in vitro* and *in vivo* screening. However, understanding this mechanism will facilitate the design and streamline the discovery process. PS-ASO sequence selection and chemical modifications have dramatic effects on PS-ASO innate immune responses and PS-ASO therapeutic index. Indeed, it was reported recently that replacing a few PS with mesyl-phosphoramidate linkages significantly reduces immune responses (23). Based on mechanistic insights, further SAR studies are ongoing using a variety of chemical modifications to develop a potent PS-ASO design that limits potential side effects. These insights will be important for drug development and to help patients.

SUPPLEMENTARY DATA

Supplementary Data are available at NAR Online.

ACKNOWLEDGEMENTS

REFERENCES

1. Crooke,S.T., Liang,X.H., Crooke,R.M., Baker,B.F. and Geary,R.S. (2021) Antisense drug discovery and development technology considered in a pharmacological context. *Biochem. Pharmacol.*, **189**, 114196.
2. Crooke,S.T., Baker,B.F., Crooke,R.M. and Liang,X.H. (2021) Antisense technology: an overview and prospectus. *Nat. Rev. Drug Discov.*, **20**, 427–453.
3. Crooke,S.T., Liang,X.H., Baker,B.F. and Crooke,R.M. (2021) Antisense technology: a review. *J. Biol. Chem.*, **296**, 100416.
4. Crooke,S.T., Witztum,J.L., Bennett,C.F. and Baker,B.F. (2018) RNA-targeted therapeutics. *Cell Metab.*, **27**, 714–739.
5. Frazier,K.S. (2015) Antisense oligonucleotide therapies: the promise and the challenges from a toxicologic pathologist's perspective. *Toxicol. Pathol.*, **43**, 78–89.
6. Shen,W., De Hoyos,C.L., Migawa,M.T., Vickers,T.A., Sun,H., Low,A., Bell,T.A. 3rd, Rahdar,M., Mukhopadhyay,S., Hart,C.E. *et al.* (2019) Chemical modification of PS-ASO therapeutics reduces cellular protein-binding and improves the therapeutic index. *Nat. Biotechnol.*, **37**, 640–650.
7. Crooke,S.T., Vickers,T.A. and Liang,X.H. (2020) Phosphorothioate modified oligonucleotide-protein interactions. *Nucleic Acids Res.*, **48**, 5235–5253.
8. Gay,N.J., Symmons,M.F., Gangloff,M. and Bryant,C.E. (2014) Assembly and localization of Toll-like receptor signalling complexes. *Nat. Rev. Immunol.*, **14**, 546–558.
9. Marongiu,L., Gornati,L., Artuso,I., Zanoni,I. and Granucci,F. (2019) Below the surface: the inner lives of TLR4 and TLR9. *J Leukoc Biol*, **106**, 147–160.
10. Lind,N.A., Rael,V.E., Pestal,K., Liu,B. and Barton,G.M. (2021) Regulation of the nucleic acid-sensing Toll-like receptors. *Nat. Rev. Immunol.*, **22**, 224–235.
11. Meng,Z. and Lu,M. (2017) RNA interference-induced innate immunity, off-target effect, or immune adjuvant?*Front. Immunol.*, **8**, 331.
12. Bauer,S., Kirschning,C.J., Hacker,H., Redecke,V., Hausmann,S., Akira,S., Wagner,H. and Lipford,G.B. (2001) Human TLR9 confers responsiveness to bacterial DNA via species-specific CpG motif recognition. *Proc. Natl. Acad. Sci. U.S.A.*, **98**, 9237–9242.
13. Ohto,U., Shibata,T., Tanji,H., Ishida,H., Krayukhina,E., Uchiyama,S., Miyake,K. and Shimizu,T. (2015) Structural basis of CpG and inhibitory DNA recognition by Toll-like receptor 9. *Nature*, **520**, 702–705.
14. Ohto,U., Ishida,H., Shibata,T., Sato,R., Miyake,K. and Shimizu,T. (2018) Toll-like receptor 9 contains two DNA binding sites that function cooperatively to promote receptor dimerization and activation. *Immunity*, **48**, 649–658.
15. Rigby,R.E., Webb,L.M., Mackenzie,K.J., Li,Y., Leitch,A., Reijns,M.A., Lundie,R.J., Revuelta,A., Davidson,D.J., Diebold,S. *et al.* (2014) RNA:DNA hybrids are a novel molecular pattern sensed by TLR9. *EMBO J.*, **33**, 542–558.
16. Chan,M.P., Onji,M., Fukui,R., Kawane,K., Shibata,T., Saitoh,S., Ohto,U., Shimizu,T., Barber,G.N. and Miyake,K. (2015) DNase II-dependent DNA digestion is required for DNA sensing by TLR9. *Nat. Commun.*, **6**, 5853.
17. Babdor,J., Descamps,D., Adiko,A.C., Tohme,M., Maschalidi,S., Evnouchidou,I., Vasconcellos,L.R., De Luca,M., Mauvais,F.X., Garfa-Traore,M. *et al.* (2017) IRAP(+) endosomes restrict TLR9 activation and signaling. *Nat. Immunol.*, **18**, 509–518.
18. Combes,A., Camosseto,V., N'Guessan,P., Arguello,R.J., Mussard,J., Caux,C., Bendriss-Vermare,N., Pierre,P. and Gatti,E. (2017) BAD-LAMP controls TLR9 trafficking and signalling in human plasmacytoid dendritic cells. *Nat. Commun.*, **8**, 913.
19. Paz,S., Hsiao,J., Cauntay,P., Soriano,A., Bai,L., Machemer,T., Xiao,X., Guo,S., Hung,G., Younis,H. *et al.* (2017) The distinct and

cooperative roles of toll-like receptor 9 and receptor for advanced glycation end products in modulating in vivo inflammatory responses to select CpG and Non-CpG oligonucleotides. *Nucleic Acid Ther.*, **27**, 272–284.

20. Pirie,E., Cauntay,P., Fu,W., Ray,S., Pan,C., Lusis,A.J., Hsiao,J., Burel,S.A., Narayanan,P., Crooke,R.M. *et al.* (2019) Hybrid mouse diversity panel identifies genetic architecture associated with the acute antisense oligonucleotide-mediated inflammatory response to a 2′-O-Methoxyethyl antisense oligonucleotide. *Nucleic Acid Ther.*, **29**, 266–277.

21. Senn,J.J., Burel,S. and Henry,S.P. (2005) Non-CpG-containing antisense 2′-methoxyethyl oligonucleotides activate a proinflammatory response independent of Toll-like receptor 9 or myeloid differentiation factor 88. *J. Pharmacol. Exp. Ther.*, **314**, 972–979.

22. Drygin,D., Koo,S., Perera,R., Barone,S. and Bennett,C.F. (2005) Induction of toll-like receptors and NALP/PAN/PYPAF family members by modified oligonucleotides in lung epithelial carcinoma cells. *Oligonucleotides*, **15**, 105–118.

23. Anderson,B.A., Freestone,G.C., Low,A., De-Hoyos,C.L., Iii,W.J.D., Ostergaard,M.E., Migawa,M.T., Fazio,M., Wan,W.B., Berdeja,A. *et al.* (2021) Towards next generation antisense oligonucleotides: mesylphosphoramidate modification improves therapeutic index and duration of effect of gapmer antisense oligonucleotides. *Nucleic Acids Res.*, **49**, 9026–9041.

24. Park,B., Buti,L., Lee,S., Matsuwaki,T., Spooner,E., Brinkmann,M.M., Nishihara,M. and Ploegh,H.L. (2011) Granulin is a soluble cofactor for toll-like receptor 9 signaling. *Immunity*, **34**, 505–513.

25. Ivanov,S., Dragoi,A.M., Wang,X., Dallacosta,C., Louten,J., Musco,G., Sitia,G., Yap,G.S., Wan,Y., Biron,C.A. *et al.* (2007) A novel role for HMGB1 in TLR9-mediated inflammatory responses to CpG-DNA. *Blood*, **110**, 1970–1981.

26. Tian,J., Avalos,A.M., Mao,S.Y., Chen,B., Senthil,K., Wu,H., Parroche,P., Drabic,S., Golenbock,D., Sirois,C. *et al.* (2007) Toll-like receptor 9-dependent activation by DNA-containing immune complexes is mediated by HMGB1 and RAGE. *Nat. Immunol.*, **8**, 487–496.

27. Gaus,H.J., Gupta,R., Chappell,A.E., Ostergaard,M.E., Swayze,E.E. and Seth,P.P. (2019) Characterization of the interactions of chemically-modified therapeutic nucleic acids with plasma proteins using a fluorescence polarization assay. *Nucleic Acids Res.*, **47**, 1110–1122.

28. Liang,X.H., Shen,W., Sun,H., Prakash,T.P. and Crooke,S.T. (2014) TCP1 complex proteins interact with phosphorothioate oligonucleotides and can co-localize in oligonucleotide-induced nuclear bodies in mammalian cells. *Nucleic. Acids. Res.*, **42**, 7819–7832.

29. Pollak,A., Cauntay,P., Machemer,T., Paz,S., Damle,S., Henry,S. and Burel,S. (2021) Mechanism driven early stage identification and avoidance of antisense oligonucleotides causing TRL9 mediated inflammatory responses in bjab cells. bioRxiv doi: https://doi.org/10.1101/2021.12.12.472280, 14 December 2021, preprint: not peer reviewed.

30. Liang,X.H., Sun,H., Nichols,J.G., Allen,N., Wang,S., Vickers,T.A., Shen,W., Hsu,C.W. and Crooke,S.T. (2018) COPII vesicles can affect the activity of antisense oligonucleotides by facilitating the release of oligonucleotides from endocytic pathways. *Nucleic Acids Res.*, **46**, 10225–10245.

31. Vickers,T.A. and Crooke,S.T. (2016) Development of a quantitative BRET affinity assay for nucleic acid-protein interactions. *PLoS One*, **11**, e0161930.

32. Alharbi,A.S., Garcin,A.J., Lennox,K.A., Pradeloux,S., Wong,C., Straub,S., Valentin,R., Pepin,G., Li,H.M., Nold,M.F. *et al.* (2020) Rational design of antisense oligonucleotides modulating the activity of TLR7/8 agonists. *Nucleic Acids Res.*, **48**, 7052–7065.

33. Al-Bari,M.A. (2015) Chloroquine analogues in drug discovery: new directions of uses, mechanisms of actions and toxic manifestations

from malaria to multifarious diseases. *J. Antimicrob. Chemother.*, **70**, 1608–1621.

34. Crooke,S.T., Wang,S., Vickers,T.A., Shen,W. and Liang,X.H. (2017) Cellular uptake and trafficking of antisense oligonucleotides. *Nat. Biotechnol.*, **35**, 230–237.

35. Liang,X.H., Shen,W., Sun,H., Kinberger,G.A., Prakash,T.P., Nichols,J.G. and Crooke,S.T. (2016) Hsp90 protein interacts with phosphorothioate oligonucleotides containing hydrophobic 2′-modifications and enhances antisense activity. *Nucleic Acids Res.*, **44**, 3892–3907.

36. Avalos,A.M. and Ploegh,H.L. (2011) Competition by inhibitory oligonucleotides prevents binding of CpG to C-terminal TLR9. *Eur. J. Immunol.*, **41**, 2820–2827.

37. Pohar,J., Lainscek,D., Ivicak-Kocjan,K., Cajnko,M.M., Jerala,R. and Bencina,M. (2017) Short single-stranded DNA degradation products augment the activation of Toll-like receptor 9. *Nat. Commun.*, **8**, 15363.

38. Pohar,J., Kuznik Krajnik,A., Jerala,R. and Bencina,M. (2015) Minimal sequence requirements for oligodeoxyribonucleotides activating human TLR9. *J. Immunol.*, **194**, 3901–3908.

39. Pohar,J., Yamamoto,C., Fukui,R., Cajnko,M.M., Miyake,K., Jerala,R. and Bencina,M. (2017) Selectivity of human TLR9 for double CpG motifs and implications for the recognition of genomic DNA. *J. Immunol.*, **198**, 2093–2104.

40. Valentin,R., Wong,C., Alharbi,A.S., Pradeloux,S., Morros,M.P., Lennox,K.A., Ellyard,J.I., Garcin,A.J., Ullah,T.R., Kusuma,G.D. *et al.* (2021) Sequence-dependent inhibition of cGAS and TLR9 DNA sensing by 2′-O-methyl gapmer oligonucleotides. *Nucleic Acids Res.*, **49**, 6082–6099.

41. Casulleras,M., Flores-Costa,R., Duran-Guell,M., Alcaraz-Quiles,J., Sanz,S., Titos,E., Lopez-Vicario,C., Fernandez,J., Horrillo,R., Costa,M. *et al.* (2020) Albumin internalizes and inhibits endosomal TLR signaling in leukocytes from patients with decompensated cirrhosis. *Sci. Transl. Med.*, **12**, eaax5135.

42. Bartneck,M., Fech,V., Ehling,J., Govaere,O., Warzecha,K.T., Hittatiya,K., Vucur,M., Gautheron,J., Luedde,T., Trautwein,C. *et al.* (2016) Histidine-rich glycoprotein promotes macrophage activation and inflammation in chronic liver disease. *Hepatology*, **63**, 1310–1324.

43. Vogl,T., Stratis,A., Wixler,V., Voller,T., Thurainayagam,S., Jorch,S.K., Zenker,S., Dreiling,A., Chakraborty,D., Frohling,M. *et al.* (2018) Autoinhibitory regulation of S100A8/S100A9 alarmin activity locally restricts sterile inflammation. *J. Clin. Invest.*, **128**, 1852–1866.

44. Wang,S., Song,R., Wang,Z., Jing,Z., Wang,S. and Ma,J. (2018) S100A8/A9 in inflammation. *Front. Immunol.*, **9**, 1298.

45. Roberts,T.L., Dunn,J.A., Sweet,M.J., Hume,D.A. and Stacey,K.J. (2011) The immunostimulatory activity of phosphorothioate CpG oligonucleotides is affected by distal sequence changes. *Mol. Immunol.*, **48**, 1027–1034.

46. Zhang,Z., Ohto,U., Shibata,T., Krayukhina,E., Taoka,M., Yamauchi,Y., Tanji,H., Isobe,T., Uchiyama,S., Miyake,K. *et al.* (2016) Structural analysis reveals that Toll-like receptor 7 is a dual receptor for guanosine and single-stranded RNA. *Immunity*, **45**, 737–748.

47. Zhang,Z., Ohto,U. and Shimizu,T. (2017) Toward a structural understanding of nucleic acid-sensing Toll-like receptors in the innate immune system. *FEBS Lett.*, **591**, 3167–3181.

48. Jameson,S.C. and Bevan,M.J. (1995) T cell receptor antagonists and partial agonists. *Immunity*, **2**, 1–11.

49. Hanes,M.S., Salanga,C.L., Chowdry,A.B., Comerford,I., McColl,S.R., Kufareva,I. and Handel,T.M. (2015) Dual targeting of the chemokine receptors CXCR4 and ACKR3 with novel engineered chemokines. *J. Biol. Chem.*, **290**, 22385–22397.

50. Li,Y., Berke,I.C. and Modis,Y. (2012) DNA binding to proteolytically activated TLR9 is sequence-independent and enhanced by DNA curvature. *EMBO J.*, **31**, 919–931.

51. Austermann,J., Spiekermann,C. and Roth,J. (2018) S100 proteins in rheumatic diseases. *Nat Rev Rheumatol*, **14**, 528–541.